Molecular Cell
Article

Identification of a BRCA1-mRNA Splicing Complex Required for Efficient DNA Repair and Maintenance of Genomic Stability

Kienan I. Savage,[1,*] Julia J. Gorski,[1] Eliana M. Barros,[1] Gareth W. Irwin,[1] Lorenzo Manti,[2] Alexander J. Powell,[1] Andrea Pellagatti,[5] Natalia Lukashchuk,[6] Dennis J. McCance,[1] W. Glenn McCluggage,[1,4] Giuseppe Schettino,[1,7] Manuel Salto-Tellez,[1] Jacqueline Boultwood,[5] Derek J. Richard,[3] Simon S. McDade,[1] and D. Paul Harkin[1,*]
[1]Centre for Cancer Research and Cell Biology, Queen's University Belfast, 97 Lisburn Road, Belfast BT9 7BL, UK
[2]Dipartimento di Fisiche, Università Federico II di Napoli, Complesso Universitario di Monte S. Angelo, Naples 80126, Italy
[3]Institute of Health and Biomedical Innovation, Queensland University of Technology, 60 Musk Avenue, Kelvin Grove, 4059 Brisbane, Australia
[4]Department of Pathology, Belfast Health and Social Care Trust, 274 Grosvenor Road, Belfast BT12 6BA, UK
[5]Leukaemia and Lymphoma Research Molecular Haematology Unit, Nuffield Department of Clinical Laboratory Sciences, John Radcliffe Hospital, Oxford OX3 9DU, UK
[6]The Gurdon Institute and Department of Biochemistry, University of Cambridge, Tennis Court Road, Cambridge CB2 1QN, UK
[7]Radiation Dosimetry Group, National Physical Laboratory, Hampton Road, Teddington TW11 0LW, UK
*Correspondence: k.savage@qub.ac.uk (K.I.S.), d.harkin@qub.ac.uk (D.P.H.)
http://dx.doi.org/10.1016/j.molcel.2014.03.021

SUMMARY

Mutations within *BRCA1* predispose carriers to a high risk of breast and ovarian cancers. BRCA1 functions to maintain genomic stability through the assembly of multiple protein complexes involved in DNA repair, cell-cycle arrest, and transcriptional regulation. Here, we report the identification of a DNA damage-induced BRCA1 protein complex containing BCLAF1 and other key components of the mRNA-splicing machinery. In response to DNA damage, this complex regulates pre-mRNA splicing of a number of genes involved in DNA damage signaling and repair, thereby promoting the stability of these transcripts/proteins. Further, we show that abrogation of this complex results in sensitivity to DNA damage, defective DNA repair, and genomic instability. Interestingly, mutations in a number of proteins found within this complex have been identified in numerous cancer types. These data suggest that regulation of splicing by the BRCA1-mRNA splicing complex plays an important role in the cellular response to DNA damage.

INTRODUCTION

The DNA damage response (DDR) pathway has evolved to protect cells from both endogenous and exogenous sources of DNA damage and ultimately to prevent tumorigenic transformation. One of the key players in the DDR pathway is BRCA1. Heterozygous mutations within BRCA1 predispose carriers to a high risk of breast and ovarian cancer (Savage and Harkin, 2009). BRCA1 functions to maintain genomic stability and plays key roles in cell-cycle checkpoint activation, homologous recombination (HR)-mediated DNA double-strand break (DSB) repair, and transcriptional regulation (Savage and Harkin, 2009). BRCA1 broadly functions as a scaffolding protein, facilitating the assembly of multiple and distinct multiprotein complexes, with various functions within the DDR. The formation and function of these complexes are thought to be regulated by phosphorylation of BRCA1 by the ATM, ATR, and Chk2 kinases in response to DNA damage, and a number of BRCA1 functions have been attributed to these phosphorylation events. For example, DNA damage-induced phosphorylation of BRCA1 serine-1423 and serine-1524 by ATM or ATR is required for resistance to ionizing radiation (IR) and G1/S and G2/M-phase arrest, respectively, whereas phosphorylation of serine-1387 is specifically required for intra-S phase arrest (Cortez et al., 1999). However, despite the broad functions associated with different BRCA1 phosphorylation sites, the mechanistic role(s) of specific DNA damage-induced BRCA1 phosphorylation events remains largely unknown.

Here we identify a DNA damage-induced BRCA1 binding protein, BCLAF1, which mediates the formation of a BRCA1-mRNA splicing complex following DNA damage. We show that through this interaction with BCLAF1, BRCA1, which is constitutively bound to a subset of genes, recruits the mRNA splicing machinery, resulting in enhanced pre-mRNA splicing of BRCA1/BCLAF1 target genes, thereby promoting transcript stability and protein expression. Intriguingly, many of the genes/proteins regulated by the BRCA1/BCLAF1 complex are involved in the DDR, and depletion of BRCA1, BCLAF1, and other members of the BRCA1-mRNA splicing complex (U2AF65) results in sensitivity to DNA damage and defective DNA repair.

RESULTS

Identification of BCLAF1 as a BRCA1^{pSer1423}-Interacting Protein

To examine how DNA damage-induced BRCA1 phosphorylation events might mechanistically regulate associated BRCA1 functions, we performed phosphopeptide pull-down assays

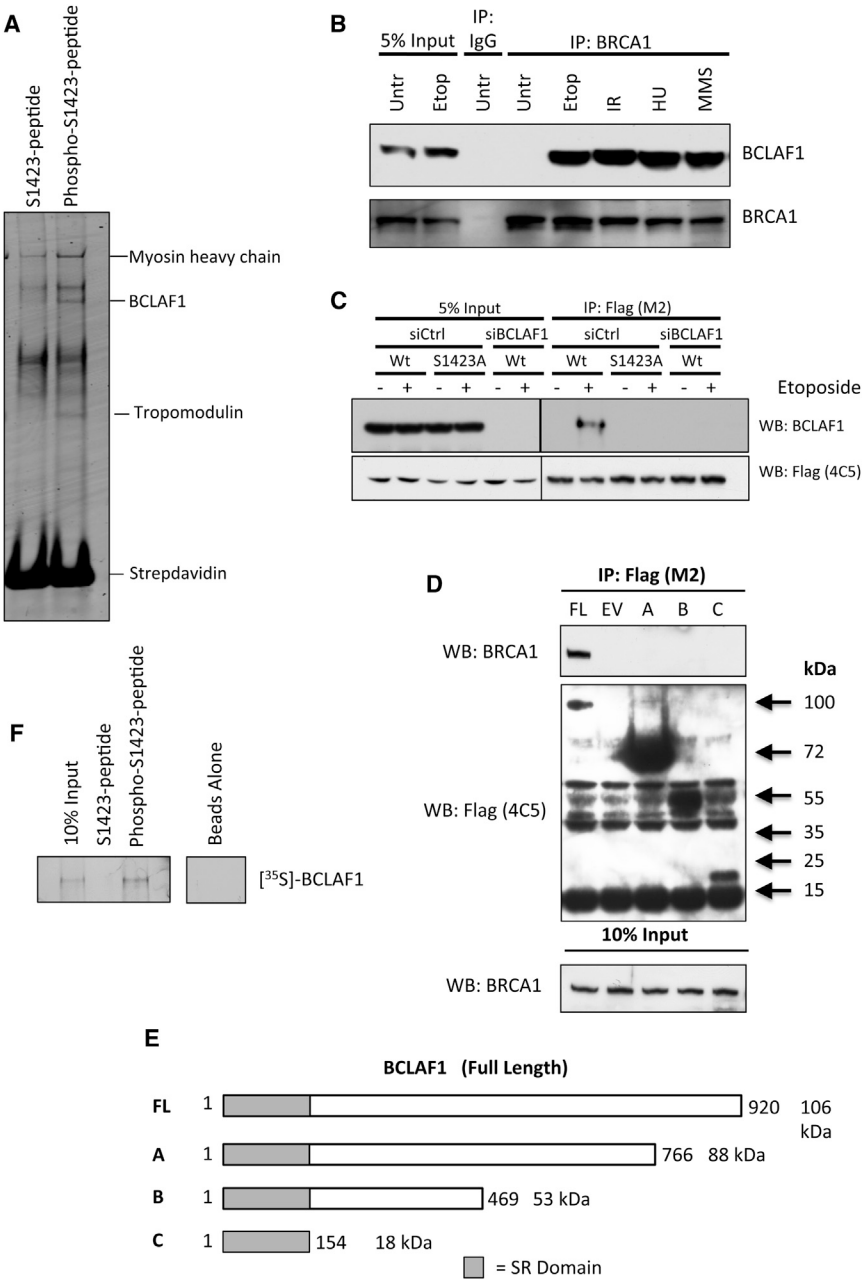

Figure 1. BCLAF1 Interacts with Phosphorylated BRCA1 following DNA Damage

(A) Colloidal Coomassie-stained gel of peptide pull-down assays carried out from 293T cell nuclear extracts with phosphorylated BRCA1-S1423 peptide and its nonphosphorylated counterpart. The indicated phosphopeptide-interacting band was identified as BCLAF1 by LC-MS/MS.

(B) Coimmunoprecipitation assay demonstrating an interaction between BRCA1 and BCLAF1 in 293T cells treated with etoposide (1 μM, 16 hr), IR (2 Gy, 1 hr), MMS (200 μM, 6 hr), and HU (5 μM, 3 hr).

(C) Coimmunoprecipitation assay demonstrating DNA damage-induced interaction of BCLAF1 with ectopic Flag-BRCA1 is abrogated by BRCA1-S1423A phosphosite substitution. A Flag-BRCA1 IP was also carried out from cells depleted of BCLAF1 to confirm the specificity of the BCLAF1 antibody.

(D) Mapping of the BRCA1-interacting region within BCLAF1. Coimmunoprecipitation experiments were carried out from etoposide-treated cells transfected with the Flag-BCLAF1 truncation mutant constructs depicted in (E).

(E) Schematic diagram of BCLAF1 truncation constructs used for BRCA1 coimmunoprecipitation experiments in (D).

(F) Peptide pull-down assays carried out with [^{35}S] in vitro-translated BCLAF1, indicating that BCLAF1 interacts directly and specifically with the phosphorylated BRCA1-S1423 peptide and not its unphosphorylated counterpart. See also Figure S1.

followed by LC-MS/MS, to identify phospho-BRCA1-interacting proteins. Using this approach, we identified BCLAF1 as a BRCA1 phosphoserine-1423 (pSer-1423)-interacting protein (Figure 1A and see Figure S1A available online). Coimmunoprecipitation confirmed that BCLAF1 interacts with BRCA1 in response to DNA alkylation (MMS), stalled replication forks (HU), and DNA double-strand breaks (IR and etoposide) and is not mediated indirectly through RNA/DNA bridging (Figures 1B, S1B, and S1C). This suggests that this complex forms as part of a general DDR mechanism and is likely a reflection of BRCA1$^{Ser-1423}$ being a substrate of both ATM and ATR, which are activated in response to DSBs or DNA single-strand breaks/stalled replication forks, respectively. In keeping with this, substitution of BRCA1$^{Ser-1423}$ with alanine abrogated the damage-induced interaction between BRCA1 and BCLAF1, confirming BCLAF1 as a BRCA1$^{pSer-1423}$ interacting protein (Figure 1C). Coimmunoprecipitation experiments with a series of Flag-tagged BCLAF1 truncated proteins (harvested from etoposide treated cells) revealed that deletion of the C-terminal region of BCLAF1 abolishes its ability to interact with BRCA1 (Figures 1D and 1E). The C terminus of BCLAF1 contains no defined domains, though it is positively charged under physiological conditions (pI = ~9.5), suggesting that the interaction between BRCA1$^{pSer-1423}$ and the BCLAF1 C terminus may occur directly. Consistent with this, in vitro-translated BCLAF1 bound strongly to the phosphorylated Ser1423-BRCA1 peptide, but not its nonphosphorylated counterpart (Figures 1F and S1D).

BCLAF1 Promotes Resistance to DNA Damage and Is Required for Efficient DNA Repair and Maintenance of Genomic Stability

BCLAF1 was first identified as a *Bcl2*-associated transcription factor that promotes apoptosis. Further studies found that BCLAF1 binds the *TP53* promoter in response to Adriamycin

treatment, where it is required for PKC-delta-mediated *TP53* transcription and apoptosis (Liu et al., 2007). However, we and others have been unable to demonstrate a role for BCLAF1 in the regulation of *TP53* expression following DNA damage (McPherson et al., 2009). Additionally, BCLAF1 null (−/−) mice do not appear to have an altered apoptotic response; rather they exhibit immunodevelopment defects and die within 24–48 hr after birth due to gross lung malformation (McPherson et al., 2009).

BRCA1 mediates resistance to DNA-damaging agents, and phosphorylation of BRCA1$^{Ser\text{-}1423}$ has also been linked with this function (Cortez et al., 1999). Therefore, to evaluate if BCLAF1 may also play a role in this process, we assessed the effect of BCLAF1 depletion on cellular survival following DNA damage. Interestingly, BCLAF1 depletion resulted in sensitization to both IR and etoposide to an equivalent level as BRCA1 depletion (Figures 2A, 2B, and S2A). To determine whether BRCA1 and BCLAF1 promote resistance to DNA damage through a common pathway, we examined the effect of BCLAF1 depletion on cellular survival following DNA damage in the BRCA1-deficient MDA-MB-436 breast cancer cell line, which we stably transfected with an empty vector (EV) or a BRCA1 expression vector (Elstrodt et al., 2006). Surprisingly, BCLAF1 depletion did not sensitize the BRCA1-deficient MDA-MB-436-EV cells and only sensitized these cells when reconstituted with ectopic BRCA1, suggesting that BCLAF1 and BRCA1 may be epistatic, at least in mediating resistance to IR-induced DSBs (Figures S2C and S2D).

The direct role of BRCA1 in DNA DSB repair is thought to contribute strongly to its ability to promote cellular survival following DNA damage. To evaluate if BCLAF1 may also play a role in DNA repair, we assessed DNA repair kinetics in both BRCA1- and BCLAF1-depleted cells 0 and 24 hr following DNA damage. Surprisingly, like BRCA1-depleted cells, BCLAF1-depleted cells also exhibited a significant defect in their ability to resolve γ-H2AX-marked DNA breaks 24 hr after IR treatment (Figures 2C, 2D, S2D, and S2E). Moreover, depletion of BCLAF1 using an shRNA also resulted in sensitization to IR and defective DNA repair, which was rescued by ectopic expression of shRNA resistant BCLAF1 (Figures S2F–S2H). Additionally, IR-treated cells depleted of BRCA1 or BCLAF1 displayed a marked increase in chromosome aberrations in comparison to control cells, indicating that loss of BCLAF1 results in increased genomic instability following DNA damage (Figures 2E and 2F). BRCA1$^{Ser\text{-}1423}$ phosphorylation has also been linked with G1/S and G2/M checkpoint function. However, we did not observe any checkpoint defects in BCLAF1-depleted cells, suggesting that the BRCA1$^{pSer\text{-}1423}$-dependent interaction with BCLAF1 does not play a role in DNA damage-induced cell-cycle arrest (data not shown). BRCA1 plays a direct role in HR-mediated DSB repair, during which it localizes to DNA break sites. Given the dramatic DNA repair defect observed in BCLAF1-depleted cells, we examined BCLAF1 cellular localization following DNA damage. Unlike BRCA1, we found that BCLAF1 was excluded from DNA break sites induced by laser microirradiation (Figure S2I).

Similar findings were recently reported for BCLAF1 and THRAP3, a protein sharing 48% identity with BCLAF1 and which has also been identified as a DNA damage-induced ATM/ATR phosphorylation substrate (Beli et al., 2012). BCLAF1 and THRAP3 associate within a complex containing a number of mRNA processing proteins, which promotes the efficient splicing of Cyclin-D1 pre-mRNAs, functioning to generate stable postspliced Cyclin-D1 transcripts (Bracken et al., 2008). In support of a role in mRNA splicing/processing, Beli et al. found that exclusion of THRAP3 and associated factors such as BCLAF1 from DNA break sites was concomitant with inhibition of transcription and subsequent loss of mRNA processing at sites of DNA damage mediated by ATM/ATR/DNA-PK (Beli et al., 2012). Taken together, these findings support a role for BCLAF1 in mRNA processing/splicing and suggest that, unlike BRCA1, BCLAF1's role in DNA repair is likely to be indirect.

BRCA1/BCLAF1 Interaction Mediates the Formation of a BRCA1-mRNA Splicing Complex, which Drives the Splicing of a Subset of Genes following DNA Damage

BCLAF1 contains a Serine-Arginine (SR) rich region within its N terminus, which is consistent with a role in pre-mRNA processing and/or splicing (Cáceres et al., 1997). In addition, as mentioned above, BCLAF1 has been shown to form part of an mRNA splicing/processing complex required for the production of stable spliced Cyclin-D1 transcripts (Bracken et al., 2008). BCLAF1 has also been copurified with the core splicing machinery, within both spliced and unspliced human mRNP complexes, further suggesting a role in mRNA splicing (Merz et al., 2007). Indeed, when examining its subcellular localization, BCLAF1 was localized to pannuclear speckles, in both unperturbed and DNA damage-treated cells, a pattern consistent with interchromatin granule clusters formed by proteins, such as U2AF65, involved in pre-mRNA processing and splicing (Cáceres et al., 1997) (Figure S2J).

Given this previously identified role for BCLAF1 in pre-mRNA splicing and interaction with a number of core splicing machinery proteins, we examined the ability of BCLAF1 and BRCA1 to interact with known components of the BCLAF1 interacting spliceosome (Merz et al., 2007). Coimmunoprecipitation confirmed that BCLAF1 constitutively interacts with a number of these core mRNA splicing proteins such as Prp8, U2AF65, U2AF35, and SF3B1, independently of DNA damage (Figure 3A). In contrast, BRCA1 coprecipitated with Prp8, U2AF65, U2AF35, and SF3B1 only in response to DNA damage (Figure 3B). Furthermore, depletion of BCLAF1 resulted in abrogation of the damage-induced interaction between BRCA1 and these proteins, suggesting that BCLAF1 mediates the interaction between phosphorylated BRCA1 and core components of the spliceosome in response to DNA damage (Figure 3B).

We have previously demonstrated that BRCA1 is bound to a large subset of gene promoters throughout the genome, though it does not regulate the transcription of the majority of these genes in unperturbed cells (Gorski et al., 2011). However, in response to various stresses, such as DNA damage, expression of many of these genes is regulated in a BRCA1-dependent manner. BRCA1$^{Ser\text{-}1423}$ phosphorylation is thought to occur at DNA break sites, where it colocalizes with active ATM/ATR. In contrast, we and others have observed that BCLAF1, which only interacts with BRCA1$^{pSer\text{-}1423}$, is excluded from DNA break

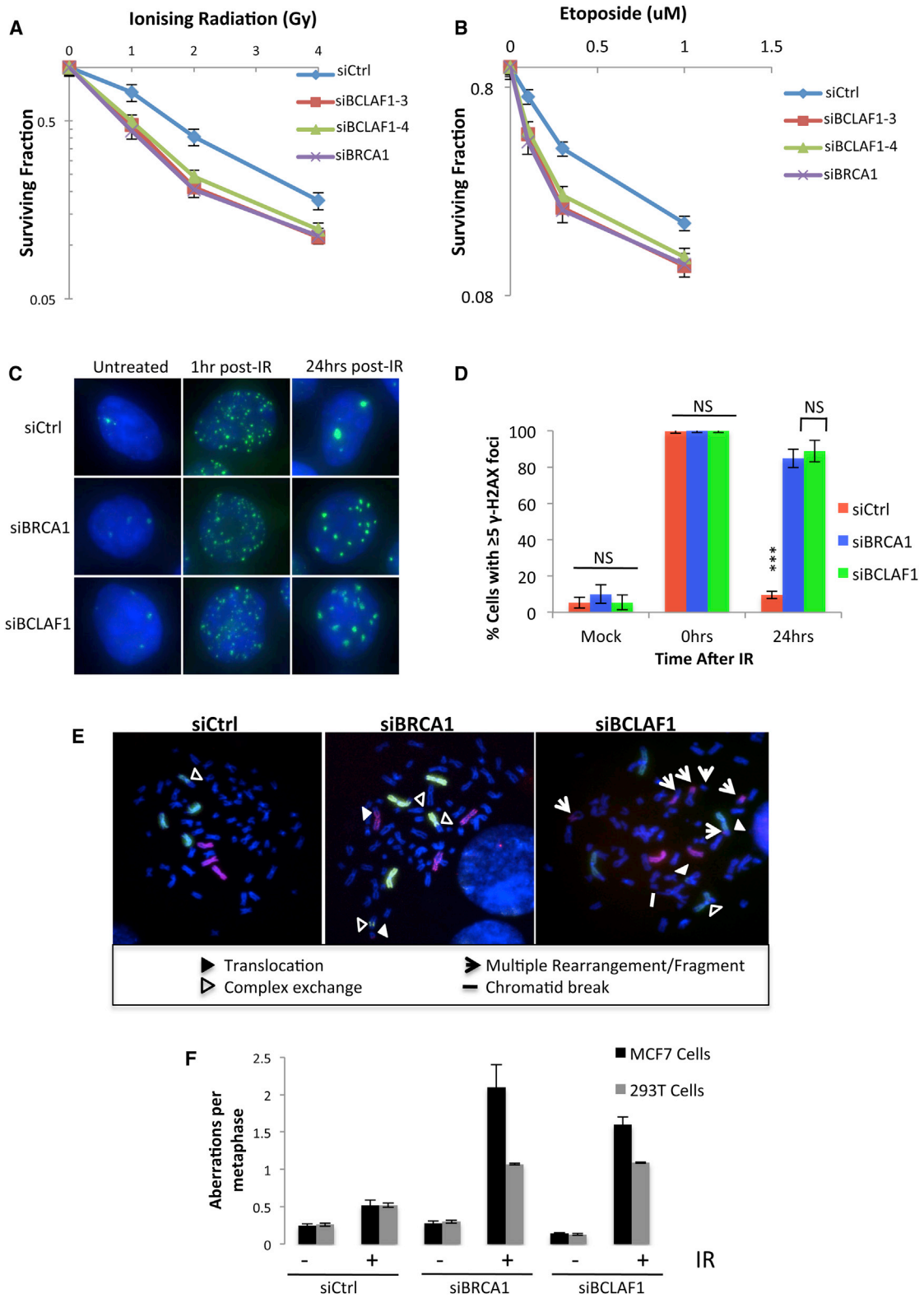

Figure 2. BRCA1/BCLAF1 Mediates Resistance to DNA Damage and Is Required for Efficient DNA Repair and Maintenance of Genomic Stability
(A and B) Clonogenic survival assays demonstrating that depletion of BRCA1 or BCLAF1 (two independent siRNAs) induces sensitivity to ionizing radiation (IR) and etoposide in (MCF7) cells. Mean surviving fraction of three independent experiments is plotted ± SEM.

(legend continued on next page)

sites (Beli et al., 2012). Therefore, to examine whether BRCA1$^{Ser-1423}$ phosphorylation is restricted to DNA break sites, or may occur on BRCA1 bound to chromatin more globally, we performed high-resolution confocal microscopy with BRCA1$^{pSer-1423}$ antibodies on cells following extraction of non-chromatin-bound proteins. As expected, this revealed that BRCA1$^{pSer-1423}$ is concentrated at DNA break sites (marked by γ-H2AX) but also revealed the presence of chromatin bound BRCA1$^{pSer-1423}$ throughout the nucleus, which was abolished by depletion of BRCA1 using specific siRNAs. This suggests that BRCA1$^{pSer-1423}$ exists in distinct chromatin bound complexes at different loci within the nucleus, which are likely to have distinct functions following DNA damage (Figure S2K).

It is well accepted that mRNA splicing occurs cotranscriptionally through the sequential recruitment of spliceosomal proteins to the chromatin/mRNA template of actively transcribed genes and is required to promote transcript maturation and stability. Therefore, we hypothesized that BRCA1, constitutively bound at gene promoters, may regulate their expression following DNA damage, through the recruitment of BCLAF1 and the cotranscriptional spliceosome, thereby promoting mRNA splicing and transcript production/stability.

In order to test this model and identify BRCA1/BCLAF1 target genes, we performed chromatin immunoprecipitation array hybridization (ChIP-chip) with BCLAF1 antibodies in unperturbed and etoposide-treated cells in the presence and absence of BRCA1 (data not shown). This strategy identified 675 genomic regions bound by BCLAF1 in response to etoposide treatment (Figure S3A). Interestingly, 610 of these regions, which mapped to 782 genes, were not bound by BCLAF1 in BRCA1-depleted cells, suggesting that, as hypothesized, BRCA1 may recruit BCLAF1 and the associated spliceosome to genetic promoter regions in order to promote cotranscriptional splicing of target genes following DNA damage (Figure S3A). Ingenuity Pathway Analysis of BRCA1/BCLAF1 regulated promoters/genes revealed that the top network involving these genes was the DNA Replication, Recombination and Repair, and Cancer network ($p = 1 \times 10^{-43}$). In keeping with this, many of these genes, such as *ATRIP*, *BACH1*, and *EXO1*, are involved in the DDR pathway, suggesting that BRCA1/BCLAF1-mediated splicing of a large subset of DDR genes may regulate cellular survival/DNA repair in response to DNA damage.

To validate ChIP-chip-identified target genes, we tested BRCA1, BCLAF1, and U2AF65 (a BCLAF1 interacting spliceosome assembly factor) binding to the promoter regions of these genes and an additional three DDR genes not identified from the ChIP-chip screen (*CHEK2*, *BRCA2*, and *ATM*) as negative controls. This confirmed that BRCA1 constitutively associates with the promoter regions of *ATRIP*, *BACH1*, and *EXO1*, in both unperturbed and etoposide-treated cells (Figures 3C and S3B–S3D). In contrast, BCLAF1 and U2AF65 binding to these regions was significantly induced upon DNA damage. As BCLAF1 only interacts with BRCA1 in response to DNA damage, we tested whether BRCA1 is required for BCLAF1 recruitment to these genes. Indeed, BRCA1 depletion resulted in loss of damage-induced BCLAF1 and U2AF65 recruitment to DNA (Figures 3C and S3B–S3D). Concurrently, we also found that BRCA1 and BCLAF1 depletion resulted in loss of recruitment of U2AF65 to these promoter regions, suggesting that BRCA1-dependent recruitment of BCLAF1 mediates binding of the core splicing machinery to these genes. Importantly, we did not observe any significant binding of BRCA1, BCLAF1, or U2AF65 to the promoter regions of the negative control genes, CHEK2, BRCA2, and ATM (Figure S3E). We also found that the splicing proteins U2AF35 and SF3B1, which also interact with BRCA1 following DNA damage through interaction with BCLAF1, are recruited to these promoters following DNA damage in a BRCA1- and BCLAF1-dependent manner (Figure S3F).

Consistent with a role in cotranscriptional splicing, we also observed significant enrichment of BRCA1, BCLAF1, and U2AF65 on *ATRIP*, *BACH1*, and *EXO1* mRNA transcripts in response to DNA damage that was not evident in unperturbed cells (Figures 3D and S3G). Moreover, depletion of BRCA1 resulted in loss of BCLAF1 and U2AF65 association with these transcripts (Figures 3D and S3G). Intriguingly, depletion of BCLAF1 also resulted in loss of damage-induced BRCA1 binding, suggesting that BRCA1 does not interact directly with these mRNA transcripts but is likely associated with target transcripts through interactions with BCLAF1 and the associated mRNA binding spliceosome (Figures 3D and S3G). Additionally, we did not observe any enrichment of BRCA1, BCLAF1, or U2AF65 with *CHEK2*, *BRCA2*, or *ATM* transcripts (Figure S3H).

We also assessed binding of BRCA1, BCLAF1, and U2AF65 to a number of regions along the *ATRIP*, *BACH1*, and *EXO1* genes using ChIP-qRT-PCR. This revealed that BRCA1 constitutively binds to exonic and exon/intron boundary regions (but not intronic regions) within these genes, albeit with reduced binding associated with progression toward the 3′ end of these genes (Figures S4A–S4C). This is consistent with a role in mRNA processing/splicing, where reduced binding, with progression along genes, is associated with reduced transcript tethering concurrent with transcriptional termination. In contrast, BCLAF1 and U2AF65 were enriched at BRCA1-bound regions only following DNA damage. In support of this, examination of publically

(C) Representative immunofluorescent staining of γ-H2AX marked DNA damage in untreated 293T cells depleted of either BRCA1 or BCLAF1 and 1 and 24 hr following 2Gy IR.

(D) Quantification of three independent experiments described above (≥200 cells were scored/experiment). Mean fraction of cells containing ≥5 γ-H2AX foci is plotted ± SEM. Significant differences in the fraction of cells containing ≥5 γ-H2AX foci were assessed using Student's two-tailed t test and are indicated by ***$p < 0.001$.

(E) Representative metaphase spreads of control (siCtrl) and BRCA1- or BCLAF1-depleted 293T cells either untreated or 24 hr following 2Gy IR. FISH-mediated whole chromosome painting (chromosome 1, green; chromosome 2, red) was used to identify complex chromosome aberrations.

(F) Quantification of total chromosome aberrations in control, BRCA1, and BCLAF1 depleted 293T and MCF7 cells 24 hr after mock irradiation or irradiation with 2 Gy IR. Graphs represent the mean number of chromosome aberrations/metaphase from three independent experiments ± SEM (≥200 metaphases scored/experiment). See also Figure S2.

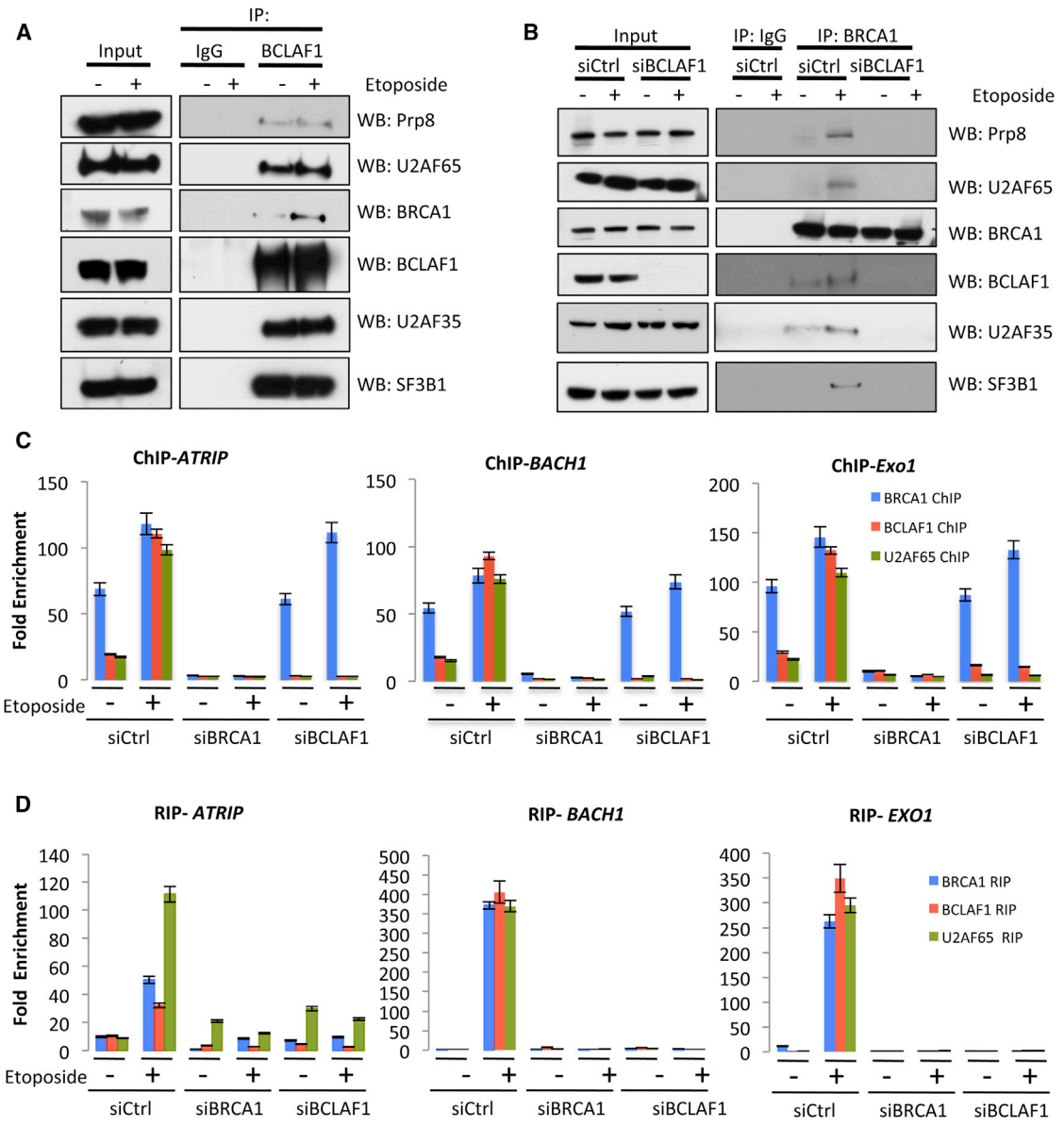

Figure 3. BRCA1/BCLAF1 Forms an mRNA Splicing Complex which Is Recruited to Target Gene Promoters and Transcripts following DNA Damage

(A) Coimmunoprecipitation assays demonstrating that BCLAF1 interacts with the spliceosome proteins Prp8, U2AF65, U2AF35, and SF3B1 in both the presence and absence of DNA damage.

(B) Coimmunoprecipitation assays demonstrating DNA damage-induced interaction between BRCA1 and the spliceosome proteins Prp8, U2AF65 U2AF35, and SF3B1 in response to DNA damage. Additionally, depletion of BCLAF1 results in abrogation of DNA damage-induced interaction between BRCA1 and these proteins.

(C) BRCA1, BCLAF1, and U2AF65 ChIP-qPCRs demonstrating constitutive binding of BRCA1 to *ATRIP*, *BACH1*, and *EXO1* promoters irrespective of DNA damage in control (siCtrl) cells. The ChIPs also demonstrate that BCLAF1 and U2AF65 are recruited to these promoters only in etoposide-treated cells and that depletion of BRCA1 or BCLAF1 results in loss of DNA damage-induced BCLAF1 and U2AF65 recruitment, respectively. Graphs represent the mean fold enrichment quantified from three independent experiments ± SEM.

(D) BRCA1, BCLAF1, and U2AF65 RIP-qRT-PCRs demonstrating that BRCA1, BCLAF1, and U2AF65 only bind to *ATRIP*, *BACH1*, and *EXO1* mRNAs in response to DNA damage. In addition, depletion of BCLAF1 results in loss of BRCA1 and U2AF65 mRNA binding to all three transcripts. Graphs represent the mean fold enrichment quantified from three independent experiments ± SEM. See also Figure S3.

available BRCA1 ChIP-seq data, derived from the normal-like breast cell line MCF10A (GEO accession number GSE40591 [Barrett et al., 2013]), also revealed BRCA1 binding across *ATRIP*, *BACH1*, and *EXO1* exons (Figures S4D and S4E). Moreover, a genome-wide analysis of all BRCA1 binding peaks within this data set revealed enrichment of BRCA1 binding peaks within

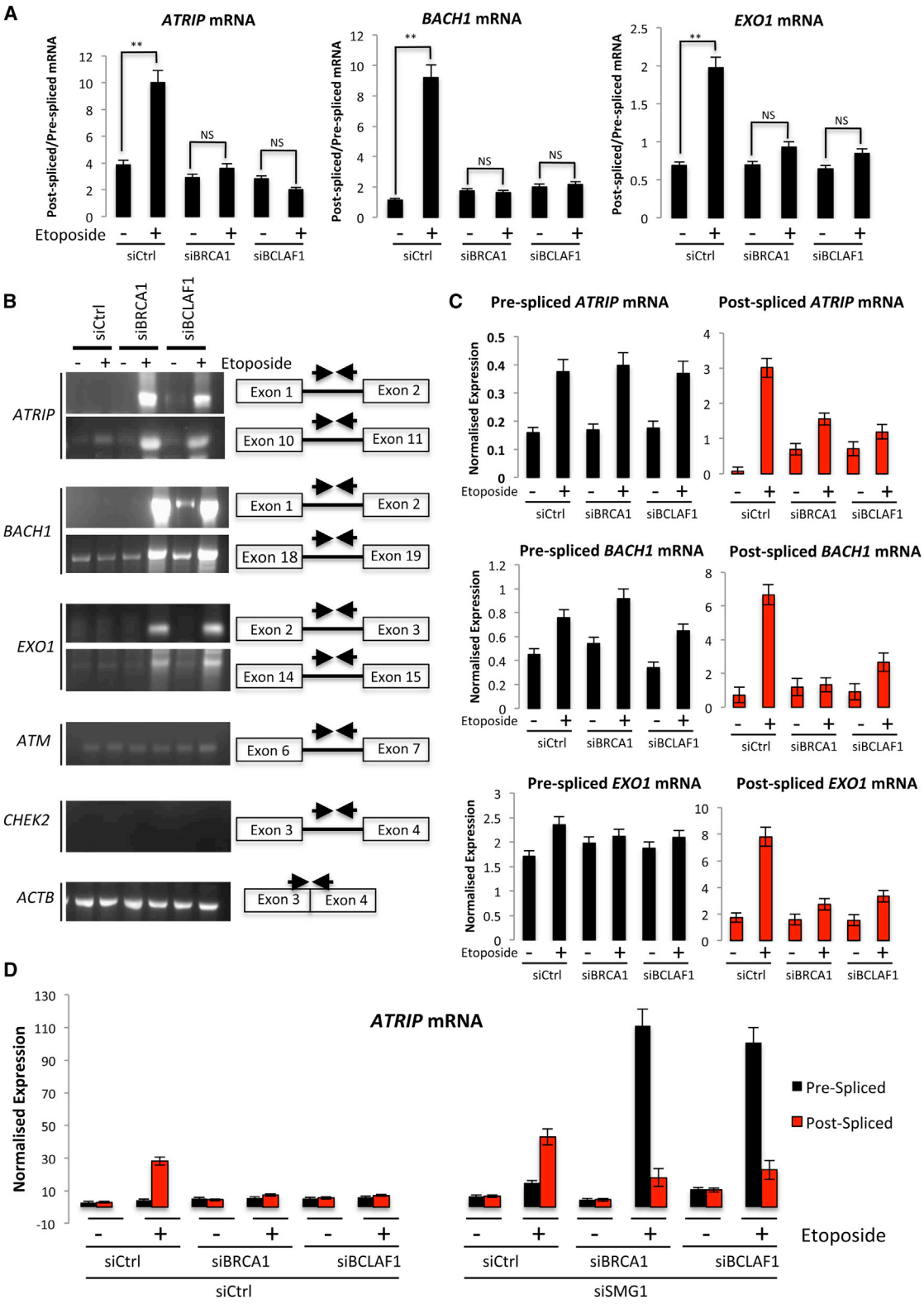

Figure 4. The BRCA1/BCLAF mRNA Splicing Complex Promotes the Splicing and Stability of *ATRIP*, *BACH1*, and *EXO1* Transcripts following DNA Damage

(A) Ratio of postspliced to prespliced *ATRIP*, *BACH1*, and *EXO1* mRNAs in control (siCtrl) and BRCA1- or BCLAF1-depleted cells mock treated or treated with etoposide. mRNA levels were assessed by qRT-PCR using exon 9-exon 10 (post-spliced-*ATRIP*) and exon 9-intron 9 (pre-spliced-*ATRIP*), exon 15-exon

(legend continued on next page)

gene promoters (and 5′ UTRs) as well as coding exons but not introns, again supporting a role for BRCA1 in mRNA splicing (Figure S4F).

Consistent with this, we found that the mRNA splicing of *ATRIP*, *BACH1*, and *EXO1* transcripts was significantly upregulated in response to DNA damage in both a BRCA1- and a BCLAF1-dependent manner using two independent siRNAs (Figures 4A and S5A). Additionally, saturating RT-PCR analysis with intron-targeted primers revealed the presence of introns in *ATRIP*, *BACH1*, and *EXO1* transcripts following DNA damage in BRCA1- and BCLAF1-depleted cells, but not control cells, confirming that splicing of these transcripts following DNA damage requires BRCA1 and BCLAF1 (Figure 4B). In response to DNA damage, transcription of *ATRIP*, *BACH1*, and *EXO1* is upregulated. However, BRCA1 or BCLAF1 depletion does not affect the transcription of these genes as indicated by similar levels of pre-mRNA production, in the absence or presence of DNA damage (Figure 4C). Similarly, RNA Pol II loading and activity on these gene promoters is unaffected by BRCA1 or BCLAF1 depletion (Figure S5B). In contrast, we observed a marked reduction in the production of postspliced *ATRIP*, *BACH1*, and *EXO1* transcripts following depletion of BRCA1 or BCLAF1 (Figure 4C). Additionally, the increased ratio of postspliced/prespliced mRNA observed in BRCA1/BCLAF1-depleted cells following DNA damage is not due to increased decay of prespliced transcripts in these cells (Figure S5C). Instead, mRNA decay experiments revealed reduced levels of postspliced *ATRIP*, *BACH1*, and *EXO1* transcripts, in comparison to prespliced transcripts, in BRCA1/BCLAF1-depleted cells following inhibition of transcription, which is consistent with a role for BRCA1/BCLAF1 in the cotranscriptional splicing of these genes (Figure S5C). Importantly, we did not observe changes in *ATRIP*, *BACH1*, or *EXO1* splice variant expression following DNA damage, suggesting that DNA damage induced BRCA1/BCLAF1-mediated splicing of these genes does not facilitate alternative splicing (data not shown).

As previously mentioned, mRNA splicing is required to maintain transcript stability, as unspliced transcripts are rapidly degraded through the non-sense-mediated decay (NMD) pathway. This likely explains why we did not observe increased levels of pre-spliced *ATRIP*, *BACH1*, or *EXO1* mRNAs after DNA damage in BRCA1- and BCLAF1-depleted cells. Consistent with this, siRNA-mediated depletion of SMG1, a key player in the NMD pathway, led to a marked increase in prespliced *ATRIP*, *BACH1*, and *EXO1* mRNAs in BRCA1- and BCLAF1-depleted cells following DNA damage (Mendell et al., 2004) (Figures 4D, S5D, and S5E).

BRCA1 Ser-1423 Phosphorylation Is Required for BCLAF1 Recruitment and Target Gene Splicing following DNA Damage

Taken together, our data suggest a model in which phosphorylated BRCA1, bound at a subset of gene promoters following DNA damage, recruits BCLAF1 and associated spliceosomal proteins, thereby facilitating DNA damage-induced mRNA splicing. To confirm that BRCA1, bound at the *ATRIP*, *BACH1*, and *EXO1* promoters, is indeed phosphorylated at serine-1423 following DNA damage, we performed ChIP-qRT-PCR with BRCA1$^{pSer\text{-}1423}$ antibodies. This revealed marked enrichment of BRCA1$^{pSer\text{-}1423}$ at the *ATRIP*, *BACH1*, and *EXO1* promoters only following DNA damage (Figure 5A). Also in support of this model, reconstitution of BRCA1 mutant cells (HCC1937) with wild-type BRCA1 restored their ability to upregulate *ATRIP*, *BACH1*, and *EXO1* mRNA splicing following DNA damage, whereas reconstitution with BRCA1^{S1423A} phosphomutant protein did not (Figures 5B–5D). Additionally, wild-type BRCA1 was able to recruit BCLAF1 to the *ATRIP*, *BACH1*, and *EXO1* promoter regions following DNA damage, whereas the BRCA1^{S1423A} phospho mutant was not (Figures 5E–5H). Consistent with this, inhibition of ATM and ATR (mediators of BRCA1^{S1423} phosphorylation) also abrogated DNA damage-induced *ATRIP*, *BACH1*, and *EXO1* mRNA splicing and recruitment of BCLAF1 and U2AF65 to their promoters (Figures S6A–S6C).

BRCA1/BCLAF1-Mediated mRNA Splicing Maintains ATRIP, BACH1, and EXO1 Protein Expression and Resistance to DNA Damage

As BRCA1 and BCLAF1 were required for efficient splicing and stability of spliced *ATRIP*, *BACH1*, and *EXO1* transcripts following DNA damage, we next assessed the effect of BRCA1 or BCLAF1 depletion on ATRIP, BACH1, and EXO1 protein expression. In keeping with the reduced expression of *ATRIP*, *BACH1*, and *EXO1* spliced transcripts, we observed substantially reduced expression of all three proteins in BRCA1- and BCLAF1-depleted cells following DNA damage (Figure 6A). However, to our surprise, in control cells we did not observe increased levels of ATRIP, BACH1, and EXO1 protein levels following DNA damage that would be expected, given the increased expression of spliced transcript observed. This suggests that either *ATRIP*, *BACH1*, and *EXO1* translation is attenuated following DNA damage or or that turnover of these proteins may be increased and that BRCA1/BCLAF1-regulated cotranscriptional splicing serves to maintain the expression of these proteins in response to DNA damage.

16 (post-spliced-*BACH1*) and exon 15-intron 15 (pre-spliced- *BACH1*), and exon 1-exon 2 (post-spliced-*EXO1*) and exon 1-intron 1 (pre-spliced- *EXO1*) primers and normalized to *ACTB* mRNA. Graphs represent the mean ratios of postspliced/prespliced mRNA from three independent experiments ± SEM. Significance of changes in splicing ratios was assessed using Student's two-tailed t test with significant changes indicated by $^{**}p < 0.01$.

(B) Semiquantitative PCR analysis of a cDNA generated from DNase-treated RNA, collected from control (siCtrl) and BRCA1- or BCLAF1-depleted cells, mock treated or treated with Etoposide. Primers targeting two independent intronic regions within *ATRIP*, *BACH1*, and *EXO1* and a single intronic region within ATM and CHEK2 (control genes) were used for semiquantitative PCR analysis. Exon-spanning primers targeted against *ACTB* were used as a loading control.

(C) Normalized expression of prespliced and postspliced mRNAs evaluated in (A).

(D) Expression levels of postspliced and prespliced *ATRIP* mRNAs in control (siCtrl) and BRCA1- or BCLAF1-depleted cells, transfected with control siRNA (siCtrl) or depleted of SMG1 (siSMG1), a key regulator of the non-sense-mediated decay pathway. Normalized expression levels were quantified as in (A). Graphs represent the mean normalized expression from three independent experiments ± SEM. See also Figures S4 and S5.

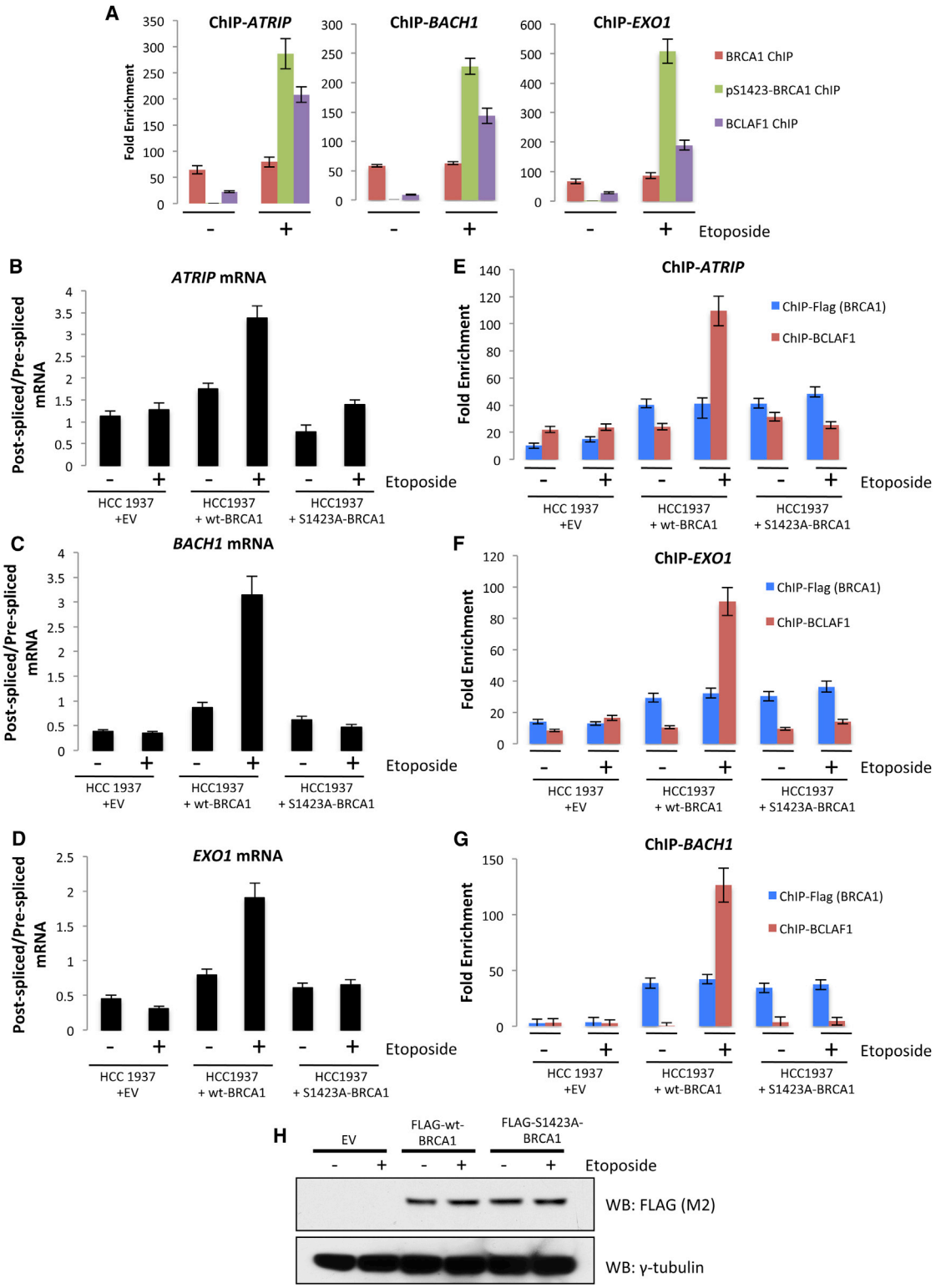

Figure 5. BRCA1 Ser-1423 Phosphorylation Is Required for BCLAF1 Recruitment and Target Gene Splicing following DNA Damage

(A) BRCA1, pS1423-BRCA1, and BCLAF1 ChIP-qPCRs demonstrating constitutive binding of BRCA1 to *ATRIP*, *BACH1*, and *EXO1* promoters irrespective of DNA damage and DNA damage-dependent enrichment of pS1423-BRCA1 and BCLAF1 on these promoters. Graphs represent the mean fold enrichment quantified from three independent experiments ± SEM.

(legend continued on next page)

To examine whether their translation is attenuated following DNA damage, we inhibited protein degradation in control and etoposide-treated cells using the proteasome inhibitor MG132. Cells were treated with etoposide for 30 min prior to MG132 treatment, after which cells were harvested at increasing time points to visualize protein production (Figure 6B). Intriguingly, ATRIP, BACH1, and EXO1 protein levels all increased more rapidly following DNA damage. This is consistent with the increased expression of spliced *ATRIP*, *BACH1*, and *EXO1* transcripts observed in these cells following DNA damage and suggests that increased turnover of these proteins is responsible for their lack of increased protein expression following DNA damage, rather than decreased translation.

To test this, we inhibited protein translation in control and etoposide-treated cells transfected with scrambled, BRCA1, or BCLAF1 targeted siRNAs using cyclohexamide. Cells were treated with etoposide for 30 min prior to cyclohexamide treatment, after which cells were harvested at increasing time points to visualize protein degradation (Figures 6C and 6D). Additionally, image densitometry was used to determine ATRIP, BACH1, and EXO1 protein half-lives (t1/2) in these cells (Figures 6E–6G). This revealed that the degradation/turnover of all three proteins was increased following DNA damage and that this was unaffected by depletion of BRCA1 or BCLAF1. Taken together, this suggests that BRCA1/BCLAF1-mediated cotranscriptional splicing and transcript stabilization serve to maintain levels of target gene proteins in response to higher rates of protein turnover following DNA damage.

Given that loss of BRCA1/BCLAF1-mediated splicing of *ATRIP*, *BACH1*, and *EXO1* results in reduced but not absent protein levels following DNA damage, we examined whether reduction of these proteins could contribute to the DNA damage sensitivity observed in BRCA1/BCLAF1-depleted cells. Indeed, reduction but not complete absence of any of these proteins, using titrated siRNA concentrations, resulted in sensitization to IR induced DNA damage (Figures S7A and S7B). In contrast, ectopic expression of ATRIP, BACH1, or EXO1 alone was unable to rescue the sensitivity of BRCA1- or BCLAF1-depleted cells to IR (data not shown). However, the combined ectopic expression of ATRIP, BACH1, and EXO1 was able to partially rescue the IR sensitivity of both BRCA1- and BCLAF1-depleted cells, suggesting that BRCA1/BCLAF1-mediated splicing of these genes is required, at least in part, for BRCA1 and BCLAF1's ability to mediate resistance to DNA damaging agents (Figures 7A and S7C).

To further confirm that the defect in DNA repair observed in BCLAF1-depleted cells is due to loss of BRCA1/BCLAF1-mediated mRNA splicing, we tested the role of U2AF65, a splicing factor recruited to target genes by BRCA1/BCLAF1, in mediating sensitivity to DNA damage and DNA repair. Indeed, U2AF65 depletion induced sensitivity to IR and defective DNA repair to a similar extent as BCLAF1 depletion (Figures 7B–7D, S7D, and S7E). Moreover, as is the case for BRCA1- and BCLAF1-depleted cells, ectopic expression of ATRIP, BACH1, and EXO1 partially rescues IR sensitivity in U2AF65-depleted cells (Figures 7E and S7F).

DISCUSSION

This study has identified a function for BRCA1 in the regulation of mRNA splicing in response to DNA damage, through the formation of a DNA damage-induced protein complex with BCLAF1, Prp8, U2AF35/65, SF3B1, and other spliceosome proteins. Consistent with this, a large, as-yet uncharacterized DNA damage-induced BRCA1 complex containing RNA and hnRNP proteins has been previously reported (Chiba and Parvin, 2001).

In addition, our data suggest that BRCA1/BCLAF1-mediated mRNA splicing in response to DNA damage may serve as a mechanism for the processing of key pre-mRNAs required for an efficient DDR and DNA repair. Intriguingly, BRCA1 has been previously reported to inhibit 3′ mRNA polyadenylation and thereby mRNA stability, through BRCA1/BARD1 ubiquitin-dependent degradation of RNA-Pol II (Kleiman et al., 2005). These studies suggest a general role for the BRCA1/BARD1 complex in blocking active transcription on a genome-wide level following DNA damage, presumably to prevent transcription of damaged genes. Despite this, it is accepted that specific genes, for example *ATRIP*, are actively transcribed in response to DNA damage, suggesting an additional mechanism that facilitates transcription/expression of a subset of genes in the context of a more genome-wide shutdown of transcription. We propose that as part of this mechanism, BRCA1 recruits the mRNA splicing machinery to a subset of promoters of genes required for an efficient DDR (such as *ATRIP*, *BACH1*, and *EXO1*), thereby promoting the cotranscriptional splicing of these genes, positively regulating the stability of their transcripts and subsequent protein expression. Intriguingly, although the BRCA1/BCLAF1 complex promoted the splicing and stability of *ATRIP*, *BACH1*, and *EXO1* transcripts following DNA damage, we did not observe an increase in the expression of these proteins in control cells, suggesting that following DNA damage the levels of these proteins may also be regulated at the translation and/or protein stability levels. When testing this, we observed no detectable change in the levels of

(B–D) Ratio of postspliced to prespliced *ATRIP*, *BACH1*, and *EXO1* mRNA in BRCA1-deficient cells (HCC1937) transfected with empty vector (EV), wild-type Flag-BRCA1 (wt-BRCA1), or S1423A Flag-BRCA1 (S1423A-BRCA1). Cells were mock treated or treated with etoposide. mRNA levels were assessed as described in Figure 4A. Graphs represent the mean ratios of postspliced/prespliced mRNA from three independent experiments ± SEM *ATRIP*, *BACH1*, and *EXO1* splicing is upregulated in cells expressing wild-type BRCA1 but not S1423A-BRCA1, indicating that phosphorylation of BRCA1 S1423 is required for DNA damage-induced splicing.

(E–G) FLAG and BCLAF1 ChIP-qRT-PCR analysis carried out in BRCA1-deficient cells (HCC1937) transfected with empty vector (EV), wild-type Flag-BRCA1 (wt), or S1423A Flag-BRCA1 (S1423A). Cells were mock treated or treated with etoposide. Graphs represent the mean fold enrichment from three independent experiments ± SEM.

(H) Representative western blots demonstrating wild-type and S1423A Flag-BRCA1 in HCC1937 cells used for splicing assays and ChIPs presented above. See also Figure S6.

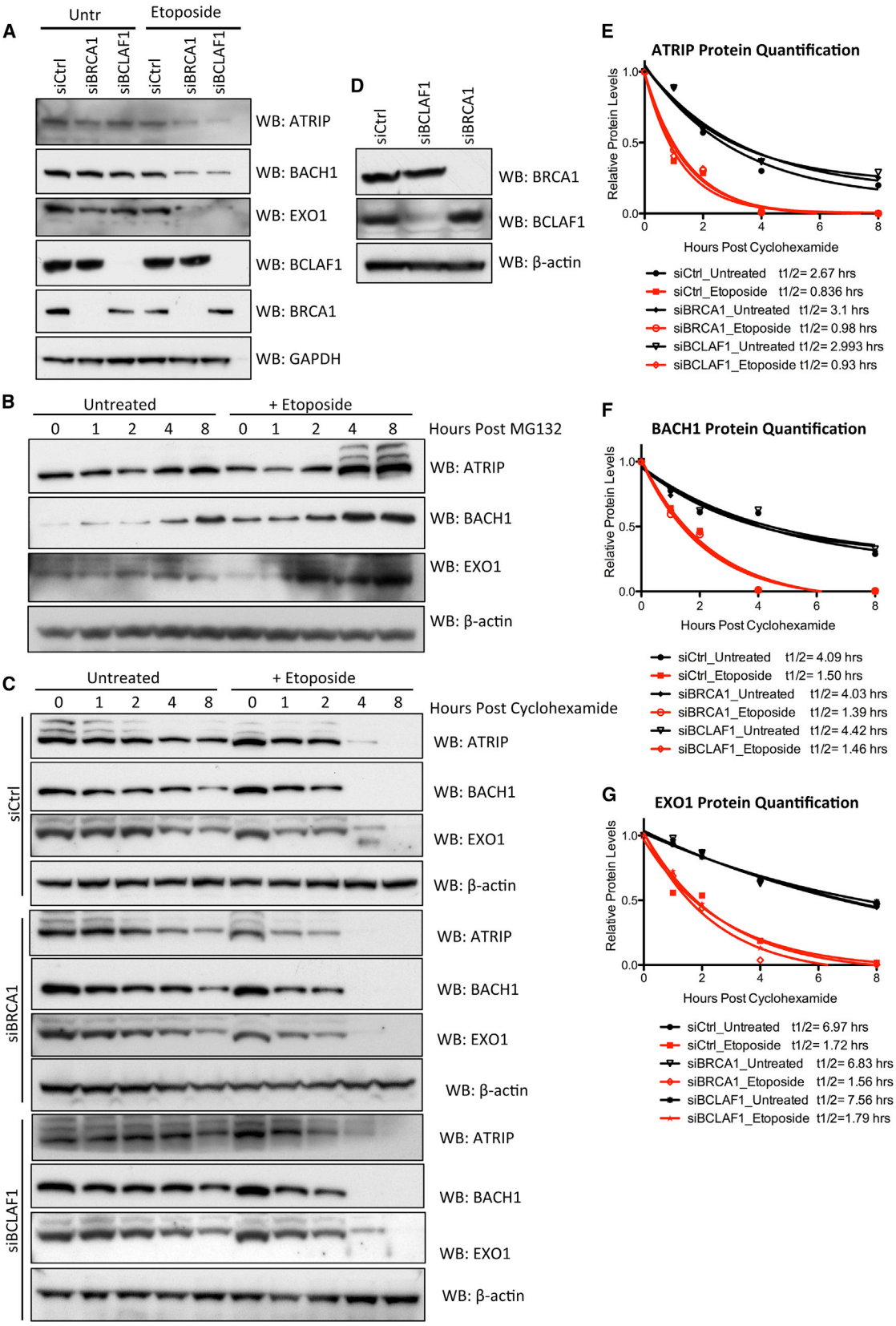

(legend on next page)

translation of these proteins following DNA damage but instead observed a dramatic increase in the rate of their turnover, suggesting that BRCA1/BCLAF1-mediated cotranscriptional splicing and transcript stabilization may serve as a mechanism through which the levels of these genes/proteins are maintained in response to higher rates of protein turnover following DNA damage. Exactly why the rate of turnover of these proteins is increased following DNA damage will require further investigation. However, it is well accepted that a number of DNA repair proteins are degraded at DNA break sites during the DNA repair process in order to facilitate removal of various proteins at different stages of repair, thereby allowing fine temporal and spatial control of repair processes. For example, KDM4A/JMJD2A is degraded through an RNF8/RNF168-dependent pathway at DNA break sites, thereby facilitating 53BP1 recruitment, loading, and subsequent repair (Mallette et al., 2012). Given that ATRIP, BACH1, and EXO1 are all recruited to DNA break sites following DNA damage, it is possible that these proteins are also degraded at break sites following DNA damage in order to facilitate ordered repair. In this context, BRCA1/BCLAF1-mediated stabilization of spliced transcripts may function in order to maintain levels of these proteins, thereby allowing the efficient repair of all DNA damage.

An intriguing finding of our study is that following DNA damage, BRCA1 and BCLAF1 interact on target gene promoters, but not at DNA break sites where BRCA1$^{pSer\text{-}1423}$ is also localized but BCLAF1 is excluded. However, it has been previously reported that exclusion of BCLAF1 and its homologous binding partner THRAP3 from DNA break sites occurs in parallel with inhibition of transcription and subsequent loss of mRNA processing at sites of DNA damage, which is mediated by ATM/ATR/DNA-PK localized at these sites (Beli et al., 2012). This suggests that after DNA damage BRCA1 plays distinct roles that require BRCA1 containing complexes at different loci: one at DNA break sites, where it is directly involved in repair (and transcription/mRNA processing is directly inhibited and BCLAF1 excluded by active ATM, ATR and/or DNA-PK), and another at transcriptionally active regions, near the promoters of DDR factors.

Surprisingly, given that the BRCA1/BCLAF1 complex regulates a relatively large pool of genes following DNA damage, we found that ectopic expression of ATRIP, BACH1, and EXO1 could partially rescue the DNA damage sensitivity phenotype of BRCA1-, BCLAF1-, and U2AF65-depleted cells, suggesting that the BRCA1/BCLAF1-mediated splicing of these genes is important for their ability to mediate resistance to DNA damage. This finding may be a reflection of the highly important role of these three proteins in the DDR, in which all play important and cooperative roles in HR-mediated DSB repair. Nevertheless, the finding that ectopic expression of these three BRCA1/BCLAF1 regulated genes only partially rescues the DNA damage sensitivity of BRCA1-, BCLAF1-, and U2AF65-depleted cells highlights that the regulation of other genes by the BRCA1/BCLAF1 complex may also be important for BRCA1/BCLAF1-mediated DNA damage resistance.

Additionally, although we have not observed BRCA1/BCLAF1-mediated alternative splicing in the genes examined in this study, it is possible that increased cotranscriptional splicing mediated by BRCA1/BCLAF1 may affect the inclusion or skipping of differential exons of regulated genes in response to DNA damage. For example, camptothecin induces increased *MDM2* cotranscriptional splicing, resulting in exon skipping and production of alternate *MDM2* splice variants (Dutertre et al., 2010). Additionally, UV-induced DNA damage has also been shown to affect cotranscriptional alternative splicing of a subset of UV-responsive genes through inhibition of RNA Pol II elongation during transcription of these genes (Muñoz et al., 2009).

Given the multiple DDR processes within which BRCA1 plays a role, in comparison to BCLAF1, another surprising finding of this study was that BCLAF1 depletion was unable to sensitize BRCA1 mutant cells to IR, as measured by clonogenic survival assays, suggesting that BRCA1 and BCLAF1 function in an epistatic manner within the same pathway. However, clonogenic survival assays only demonstrate cellular survival following a specific genotoxic insult and do not allow the functional separation of different pathways that contribute to cell death. Therefore, although demonstrating that the pathway in which BRCA1 and BCLAF1 cooperate is required for cellular survival following IR, it is unlikely that all of BRCA1's tumor-suppressive function is mediated through its role in mRNA splicing with BCLAF1 alone.

Taken together, our data suggest that the BRCA1/BCLAF1 mRNA splicing complex may act as a tumor suppressor complex, functioning to promote the splicing and stability of genes required for DNA repair and maintenance of genomic stability. In support of this, a number of SNPs within *BCLAF1* have been associated with increased risk of non-Hodgkin's lymphoma and a number of microRNAs encoded by the oncogenic Kaposi's sarcoma-associated herpes virus (KSHV) target BCLAF1, resulting in BCLAF1 depletion and sensitivity to DNA damaging agents (Kelly et al., 2010; Ziegelbauer et al., 2009). Additionally, a number of recent studies have found a high incidence of mutually

Figure 6. BRCA1/BCLAF1-Mediated mRNA Splicing Is Required for Maintenance of ATRIP, BACH1, and EXO1 Protein Expression

(A) Representative western blots demonstrating that depletion of either BRCA1 or BCLAF1 results in downregulated expression of ATRIP, BACH1, and EXO1 proteins in response to DNA damage.

(B) Representative western blot demonstrating DNA damage-dependent accumulation of ATRIP, BACH1, and EXO1 proteins over time following inhibition of proteosomal mediated protein degradation with MG132 (10 μM). Cells were mock treated or treated with etoposide (1 μM) for 30 min prior to MG132 treatment.

(C) Representative western blots demonstrating DNA damage-dependent increased protein turnover in control and BRCA1- or BCLAF1-depleted cells following inhibition of protein translation with Cyclohexamide (10 μg/mL). Cells were mock treated or treated with etoposide (1 μM) for 30 min prior to Cyclohexamide treatment.

(D) Representative western blots demonstrating BRCA1 and BCLAF depletion in cells used for experiments shown in (C).

(E–G) Quantification of ATRIP, BACH1, and EXO1 protein levels shown in (C). Image densitometry values were normalized to 0 hr and decay curves fitted and used to calculate protein half-lives.

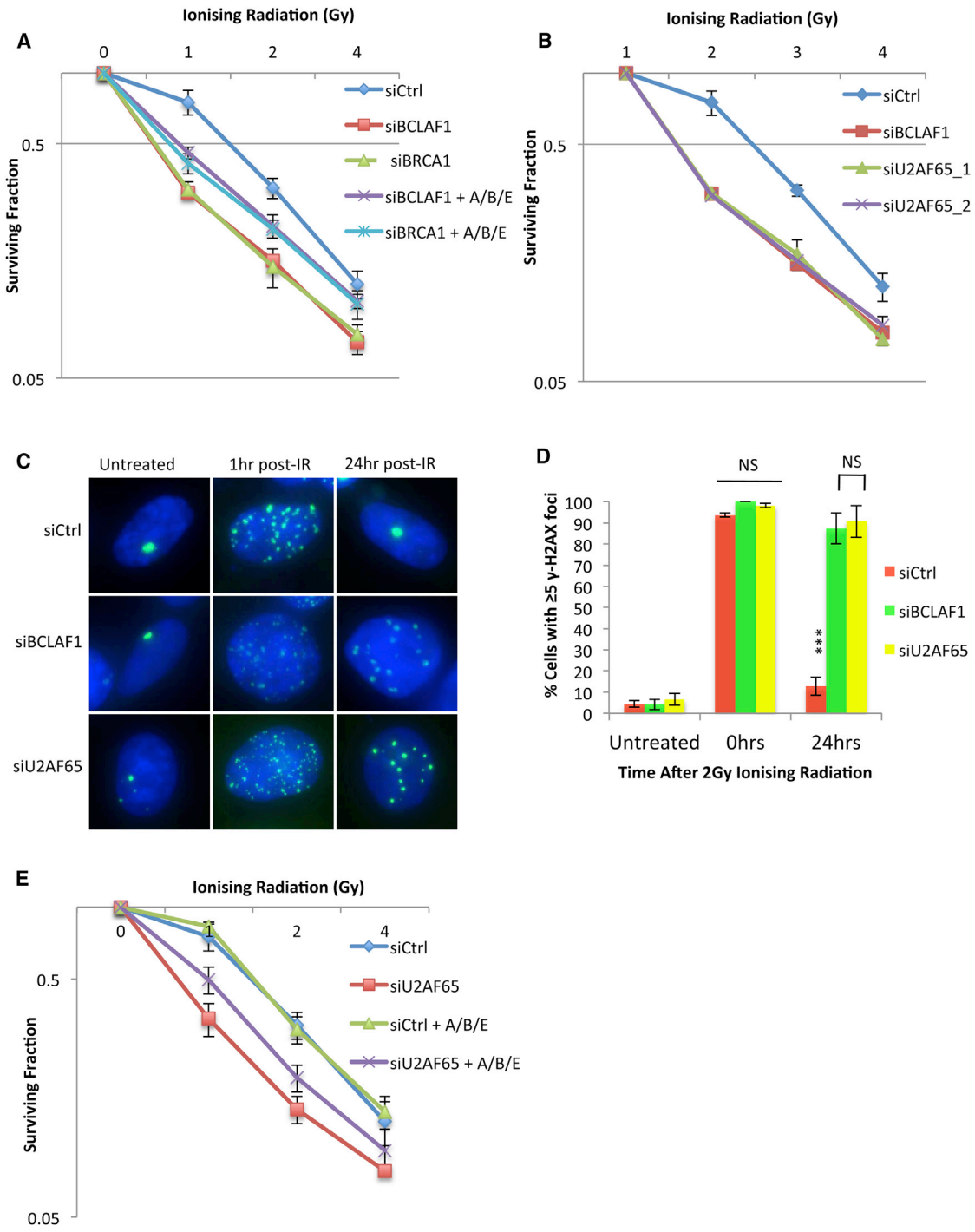

Figure 7. BRCA1/BCLAF1-Mediated mRNA Splicing of ATRIP, BACH1, and EXO1 Promotes Resistance to DNA Damage and Efficient DNA Repair

(A) Clonogenic survival assays demonstrating that ectopic expression of ATRIP, BACH1, and EXO1 (A/B/E) in BRCA1- or BCLAF1-depleted 293T cells partially rescues their sensitivity to IR. Mean surviving fraction of three independent experiments is plotted ± SEM.

(B) Clonogenic survival assays demonstrating that depletion of BCLAF1 or U2AF65 induces sensitivity to IR in 293T cells. Mean surviving fraction of three independent experiments is plotted ± SEM.

(C) Representative immunofluorescent staining of γ-H2AX marked DNA damage in untreated 293T cells depleted of either BCLAF1 or U2AF65 and 1 and 24 hr following 2Gy IR.

(legend continued on next page)

exclusive somatic mutations within members of the BRCA1/BCLAF1 mRNA splicing complex, including BCLAF1, U2AF65, U2AF35, SRSF2, SF3A1, SF3B1, and PRPF40B within various cancer types including myelodysplasia, chronic and acute myeloid leukemias, breast cancers, and lung cancers (Ding et al., 2012; Forbes et al., 2008; Merz et al., 2007; Nik-Zainal et al., 2012; Quesada et al., 2012; Yoshida et al., 2011).

Finally, given BRCA1's role in predisposition to breast and ovarian cancer, it may also be prudent to investigate the status of these genes in familial cancers not linked to BRCA1/2 mutation. Indeed, mutations within Prp22, a Prp8-interacting protein involved in pre-mRNA splicing, were previously found to cosegregate with breast and ovarian cancer (Friedman et al., 1995).

EXPERIMENTAL PROCEDURES

Cell Lines

Cell lines were obtained from the following sources: London Research Institute, London, for 293T; and ECACC for MCF7 cells. All cell lines were verified by STR profiling (ATCC-LGC Standards, Middlesex, UK).

siRNAs

siRNAs were obtained from QIAGEN. See Supplemental Information for full sequences.

Peptide Pull-Down Assays

Peptide pull-down assays were carried out as previously described (Stucki et al., 2005) using the following biotinylated peptides BRCA1-S1423: AVLEGHG**S**GPSNSYP; BRCA1-phospho-S1423: AVLEGHG**pS**GPSNSYP (Genscript).

mRNA Splicing Analysis

Introns/exons were chosen for assessment in splicing assays based on their inclusion in expressed transcripts and their suitability for optimal qRT-PCR primer design. Postspliced to prespliced *ATRIP*, *BACH1* and *EXO1* mRNA levels were quantified using qRT-PCR and normalized to *ACTB* mRNA levels. The ratio of spliced to postspliced to prespliced mRNA was then calculated by dividing the normalized expression levels of postspliced mRNAs by the normalized levels of prespliced mRNAs. See Supplemental Information for a detailed description of the methods and primer sequences used.

Clonogenic Survival Assays

Clonogenic survival assays were performed as previously described (Franken et al., 2006).

Plasmids

Flag-tagged BRCA1 construct Fl4-BRCA1 was a kind gift from Professor Richard Baer, Columbia University, New York, USA. Myc-DDK tagged ATRIP (RC223562), BACH1 (RC224085), and EXO1 (RC200547) plasmids were purchased from Origene. Plasmids were transfected with Genejuice (Merck) as per the manufacturer's instructions.

Coimmunoprecipitations

Coimmunoprecipitations were carried out as previously described using (BRCA1; Ab1, Millipore) or BCLAF1 (BTF-608A, Bethyl Laboratories) antibodies.

Western Blotting

Western blotting was performed using the invitrogen Novex system and the following antibodies: BRCA1 (D9, Santa-Cruz), BCLAF1 (BTF 608A, Bethyl Labs), U2AF65 (MC3 or H300, Santa-Cruz), Prp8 (E5, Santa-Cruz), BACH1 (4578, Cell Signaling), ATRIP (H300, Santa-Cruz), Exo1 (N18, Santa-Cruz), γ-tubulin (GTU-88, Sigma), SF3B1 (A300-996A, Bethyl Laboratories), and U2AF35 (A307-079A, Bethyl Laboratories).

Chromatin Immunoprecipitations and ChIP-Chip

Chromatin immunoprecipitations (ChIP) and ChIP-chip were carried out as previously described (Gorski et al., 2011) using the NimbleGen Human 3 × 720k RefSeq promoter array. See Supplemental Experimental Procedures for detailed protocol. Immunoprecipitated DNA was quantified by qPCR and expressed as fold enrichment over input compared to enrichment of a nonspecific negative control region. Additionally, to ensure specificity of ChIP antibodies, all ChIP experiments were accompanied by two negative control ChIPs performed with a nonspecific isotype-matched IgG and an anti-HA tag antibody. Nonspecific binding of these antibodies to DNA regions was quantified by qPCR. ChIP with these antibodies never revealed specific enrichment of any of the DNA regions quantified (data not shown).

RNA Immunoprecipitations

See Supplemental Experimental Procedures for detailed RNA immunoprecipitation (RIP) protocol. Immunoprecipitated RNA was quantified by qRT-PCR and expressed as fold enrichment over input compared to enrichment of a negative control region within the ACTB 5′ UTR. Additionally, to ensure specificity of RIP antibodies, all RIP experiments were accompanied by two negative control RIPs performed with a nonspecific isotype-matched IgG and an anti-HA tag antibody. RIP with these antibodies never revealed specific enrichment of any of the mRNA regions quantified (data not shown).

Immunofluorescent Cytochemistry

Immunofluorescent cytochemistry was carried out as previously described (Paul et al., 2011) using anti γ-H2AX, (05–636, Millipore), BCLAF1 (BTF 608A, Bethyl Labs), and U2AF65 (MC3, Santa Cruz) antibodies.

Ionising Radiation and Etoposide Treatment

Irradiations were carried out using an X-RAD 225 X-ray generator (Precision X-ray Inc. Branford, CT, USA) at a dose rate of 0.591 $Gy.min^{-1}$. Unless otherwise stated, etoposide treatments were using 1 μM for 16 hr.

Metaphase Spreads and Chromosomal Aberration Analysis

Metaphase spreads and chromosome 1 and 2 FISH were carried out as previously described (Manti et al., 2006) using XCP1 and XCP2 whole-chromosome paint probes (MetaSystems, Zeiss, Germany).

ACCESSION NUMBERS

BCLAF1 ChIP-chip data can be found at the Gene Expression Omnibus under accession number GSE47016.

SUPPLEMENTAL INFORMATION

Supplemental Information includes seven figures and Supplemental Experimental Procedures and can be found with this article at http://dx.doi.org/10.1016/j.molcel.2014.03.021.

(D. Quantification of three independent experiments described above (≥200 cells were scored/experiment). The mean fraction of cells containing ≥5 γ-H2AX foci is plotted ± SEM. Significant differences in the fraction of cells containing ≥5 γ-H2AX foci were assessed using Student's two-tailed t test and are indicated by ***$p < 0.001$.

(E) Clonogenic survival assays demonstrating that ectopic expression of ATRIP, BACH1, and EXO1 (A/B/E) in U2AF65-depleted 293T cells partially rescues their sensitivity to IR. Mean surviving fraction of three independent experiments is plotted ± SEM. See also Figure S7.

ACKNOWLEDGMENTS

This work was supported by grants from Cancer Focus Northern Ireland (K.I.S), Cancer Research UK (C538/A8132 to K.I.S., J.J.G., E.M.B., and D.P.H.), the Research and Development Office Northern Ireland (G.W.I.), the UK Medical Research Council (G0700754 to S.S.M. and D.J.M.), and the Leukaemia and Lymphoma Research of the United Kingdom (A.P. and J.B.). We would also like to thank Professor Steve Jackson (University of Cambridge) for his valuable input and discussion.

Received: September 12, 2013
Revised: December 21, 2013
Accepted: February 14, 2014
Published: April 17, 2014

REFERENCES

Barrett, T., Wilhite, S.E., Ledoux, P., Evangelista, C., Kim, I.F., Tomashevsky, M., Marshall, K.A., Phillippy, K.H., Sherman, P.M., Holko, M., et al. (2013). NCBI GEO: archive for functional genomics data sets—update. Nucleic Acids Res. *41* (Database issue), D991–D995.

Beli, P., Lukashchuk, N., Wagner, S.A., Weinert, B.T., Olsen, J.V., Baskcomb, L., Mann, M., Jackson, S.P., and Choudhary, C. (2012). Proteomic investigations reveal a role for RNA processing factor THRAP3 in the DNA damage response. Mol. Cell *46*, 212–225.

Bracken, C.P., Wall, S.J., Barré, B., Panov, K.I., Ajuh, P.M., and Perkins, N.D. (2008). Regulation of cyclin D1 RNA stability by SNIP1. Cancer Res. *68*, 7621–7628.

Cáceres, J.F., Misteli, T., Screaton, G.R., Spector, D.L., and Krainer, A.R. (1997). Role of the modular domains of SR proteins in subnuclear localization and alternative splicing specificity. J. Cell Biol. *138*, 225–238.

Chiba, N., and Parvin, J.D. (2001). Redistribution of BRCA1 among four different protein complexes following replication blockage. J. Biol. Chem. *276*, 38549–38554.

Cortez, D., Wang, Y., Qin, J., and Elledge, S.J. (1999). Requirement of ATM-dependent phosphorylation of brca1 in the DNA damage response to double-strand breaks. Science *286*, 1162–1166.

Ding, L., Ley, T.J., Larson, D.E., Miller, C.A., Koboldt, D.C., Welch, J.S., Ritchey, J.K., Young, M.A., Lamprecht, T., McLellan, M.D., et al. (2012). Clonal evolution in relapsed acute myeloid leukaemia revealed by whole-genome sequencing. Nature *481*, 506–510.

Dutertre, M., Sanchez, G., De Cian, M.C., Barbier, J., Dardenne, E., Gratadou, L., Dujardin, G., Le Jossic-Corcos, C., Corcos, L., and Auboeuf, D. (2010). Cotranscriptional exon skipping in the genotoxic stress response. Nat. Struct. Mol. Biol. *17*, 1358–1366.

Elstrodt, F., Hollestelle, A., Nagel, J.H., Gorin, M., Wasielewski, M., van den Ouweland, A., Merajver, S.D., Ethier, S.P., and Schutte, M. (2006). BRCA1 mutation analysis of 41 human breast cancer cell lines reveals three new deleterious mutants. Cancer Res. *66*, 41–45.

Forbes, S.A., Bhamra, G., Bamford, S., Dawson, E., Kok, C., Clements, J., Menzies, A., Teague, J.W., Futreal, P.A., and Stratton, M.R. (2008). The catalogue of somatic mutations in cancer (COSMIC). Curr. Protoc. Hum. Genet. *Chapter 10*, Unit 10 11.

Franken, N.A., Rodermond, H.M., Stap, J., Haveman, J., and van Bree, C. (2006). Clonogenic assay of cells in vitro. Nat. Protoc. *1*, 2315–2319.

Friedman, L.S., Ostermeyer, E.A., Lynch, E.D., Welcsh, P., Szabo, C.I., Meza, J.E., Anderson, L.A., Dowd, P., Lee, M.K., Rowell, S.E., et al. (1995). 22 genes from chromosome 17q21: cloning, sequencing, and characterization of mutations in breast cancer families and tumors. Genomics *25*, 256–263.

Gorski, J.J., Savage, K.I., Mulligan, J.M., McDade, S.S., Blayney, J.K., Ge, Z., and Harkin, D.P. (2011). Profiling of the BRCA1 transcriptome through microarray and ChIP-chip analysis. Nucleic Acids Res. *39*, 9536–9548.

Kelly, J.L., Novak, A.J., Fredericksen, Z.S., Liebow, M., Ansell, S.M., Dogan, A., Wang, A.H., Witzig, T.E., Call, T.G., Kay, N.E., et al. (2010). Germline variation in apoptosis pathway genes and risk of non-Hodgkin's lymphoma. Cancer Epidemiol. Biomarkers Prev. *19*, 2847–2858.

Kleiman, F.E., Wu-Baer, F., Fonseca, D., Kaneko, S., Baer, R., and Manley, J.L. (2005). BRCA1/BARD1 inhibition of mRNA 3′ processing involves targeted degradation of RNA polymerase II. Genes Dev. *19*, 1227–1237.

Liu, H., Lu, Z.G., Miki, Y., and Yoshida, K. (2007). Protein kinase C delta induces transcription of the TP53 tumor suppressor gene by controlling death-promoting factor Btf in the apoptotic response to DNA damage. Mol. Cell. Biol. *27*, 8480–8491.

Mallette, F.A., Mattiroli, F., Cui, G., Young, L.C., Hendzel, M.J., Mer, G., Sixma, T.K., and Richard, S. (2012). RNF8- and RNF168-dependent degradation of KDM4A/JMJD2A triggers 53BP1 recruitment to DNA damage sites. EMBO J. *31*, 1865–1878.

Manti, L., Durante, M., Grossi, G., Ortenzia, O., Pugliese, M., Scampoli, P., and Gialanella, G. (2006). Measurements of metaphase and interphase chromosome aberrations transmitted through early cell replication rounds in human lymphocytes exposed to low-LET protons and high-LET 12C ions. Mutat. Res. *596*, 151–165.

McPherson, J.P., Sarras, H., Lemmers, B., Tamblyn, L., Migon, E., Matysiak-Zablocki, E., Hakem, A., Azami, S.A., Cardoso, R., Fish, J., et al. (2009). Essential role for Bclaf1 in lung development and immune system function. Cell Death Differ. *16*, 331–339.

Mendell, J.T., Sharifi, N.A., Meyers, J.L., Martinez-Murillo, F., and Dietz, H.C. (2004). Nonsense surveillance regulates expression of diverse classes of mammalian transcripts and mutes genomic noise. Nat. Genet. *36*, 1073–1078.

Merz, C., Urlaub, H., Will, C.L., and Lührmann, R. (2007). Protein composition of human mRNPs spliced in vitro and differential requirements for mRNP protein recruitment. RNA *13*, 116–128.

Muñoz, M.J., Pérez Santangelo, M.S., Paronetto, M.P., de la Mata, M., Pelisch, F., Boireau, S., Glover-Cutter, K., Ben-Dov, C., Blaustein, M., Lozano, J.J., et al. (2009). DNA damage regulates alternative splicing through inhibition of RNA polymerase II elongation. Cell *137*, 708–720.

Nik-Zainal, S., Alexandrov, L.B., Wedge, D.C., Van Loo, P., Greenman, C.D., Raine, K., Jones, D., Hinton, J., Marshall, J., Stebbings, L.A., et al.; Breast Cancer Working Group of the International Cancer Genome Consortium (2012). Mutational processes molding the genomes of 21 breast cancers. Cell *149*, 979–993.

Paul, I., Savage, K.I., Blayney, J.K., Lamers, E., Gately, K., Kerr, K., Sheaff, M., Arthur, K., Richard, D.J., Hamilton, P.W., et al. (2011). PARP inhibition induces BAX/BAK-independent synthetic lethality of BRCA1-deficient non-small cell lung cancer. J. Pathol. *224*, 564–574.

Quesada, V., Conde, L., Villamor, N., Ordóñez, G.R., Jares, P., Bassaganyas, L., Ramsay, A.J., Beà, S., Pinyol, M., Martínez-Trillos, A., et al. (2012). Exome sequencing identifies recurrent mutations of the splicing factor SF3B1 gene in chronic lymphocytic leukemia. Nat. Genet. *44*, 47–52.

Savage, K.I., and Harkin, D.P. (2009). BRCA1 and BRCA2: role in the DNA damage response, cancer formation and treatment. In The DNA Damage Response: Implications on Cancer Formation and Treatment, Y. Shiloh and K.K. Khanna, eds. (New York: Springer), pp. 415–443.

Stucki, M., Clapperton, J.A., Mohammad, D., Yaffe, M.B., Smerdon, S.J., and Jackson, S.P. (2005). MDC1 directly binds phosphorylated histone H2AX to regulate cellular responses to DNA double-strand breaks. Cell *123*, 1213–1226.

Yoshida, K., Sanada, M., Shiraishi, Y., Nowak, D., Nagata, Y., Yamamoto, R., Sato, Y., Sato-Otsubo, A., Kon, A., Nagasaki, M., et al. (2011). Frequent pathway mutations of splicing machinery in myelodysplasia. Nature *478*, 64–69.

Ziegelbauer, J.M., Sullivan, C.S., and Ganem, D. (2009). Tandem array-based expression screens identify host mRNA targets of virus-encoded microRNAs. Nat. Genet. *41*, 130–134.

Molecular Cell, Volume *54*

Supplemental Information

Identification of a BRCA1-mRNA Splicing Complex Required for Efficient DNA Repair and Maintenance of Genomic Stability

Kienan I. Savage, Julia J. Gorski, Eliana M. Barros, Gareth W. Irwin, Lorenzo Manti, Alexander J. Powell, Andrea Pellagatti, Natalia Lukashchuk, Dennis J. McCance, W. Glenn McCluggage, Giuseppe Schettino, Manuel Salto-Tellez, Jacqueline Boultwood, Derek J. Richard, Simon S. McDade, and D. Paul Harkin

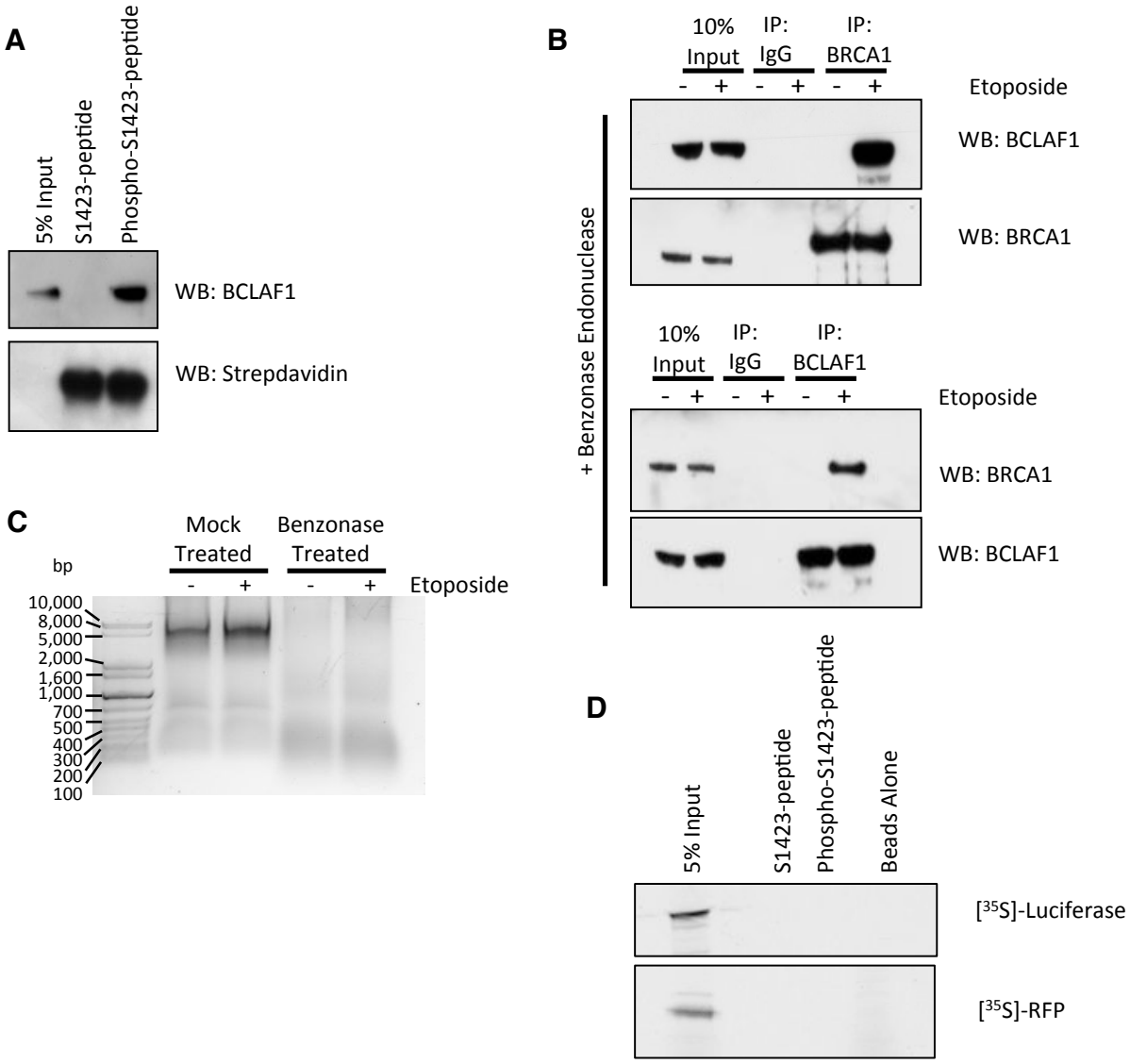

Figure S1. Interaction between BRCA1 and BCLAF1 in response to DNA damage, related to Figure 1. **A.** Immunoblot analysis of peptide pull-down assays carried out with the phosphorylated BRCA1-S1423 peptide and its unphosphorylated counterpart, from 293T nuclear extract **B.** Reciprocal co-immunoprecipitation experiments carried out from cell extracts harvested in the presence of Benzonase endonuclease which digests all nucleic acids (DNA and RNA). Co-precipitation of BRCA1 and BCLAF1 following DNA damage in Benzonase treated lysates rules out an indirect interaction between BRCA1/BCLAF1 mediated by DNA or RNA. **C.** Control for Figure S1B. Ethidium Bromide stained DNA agarose gel of protein lysates collected prior to the addition of Benzonase and following Benzonase treatment but prior to carrying out immunoprecipitation assays shown in Fig S1B. This control demonstrates complete digestion of all nucleic acids in these lysates. **D.** Control for Figure 1F. To ensure that the phospho-BRCA1 peptide does not bind non-specifically to in-vitro translated (IVT'd) proteins, peptide pull-down assays were carried out with [^{35}S] IVT'd Luciferase and Red Fluorescent protein (RFP). Neither, of the IVT'd control proteins; Luciferase or RFP, were precipitated with the unphosphorylated or phosphorylated BRCA1 -S1423 peptide, indicating that neither of these peptides interact non-specifically with IVT'd Luciferase or RFP.

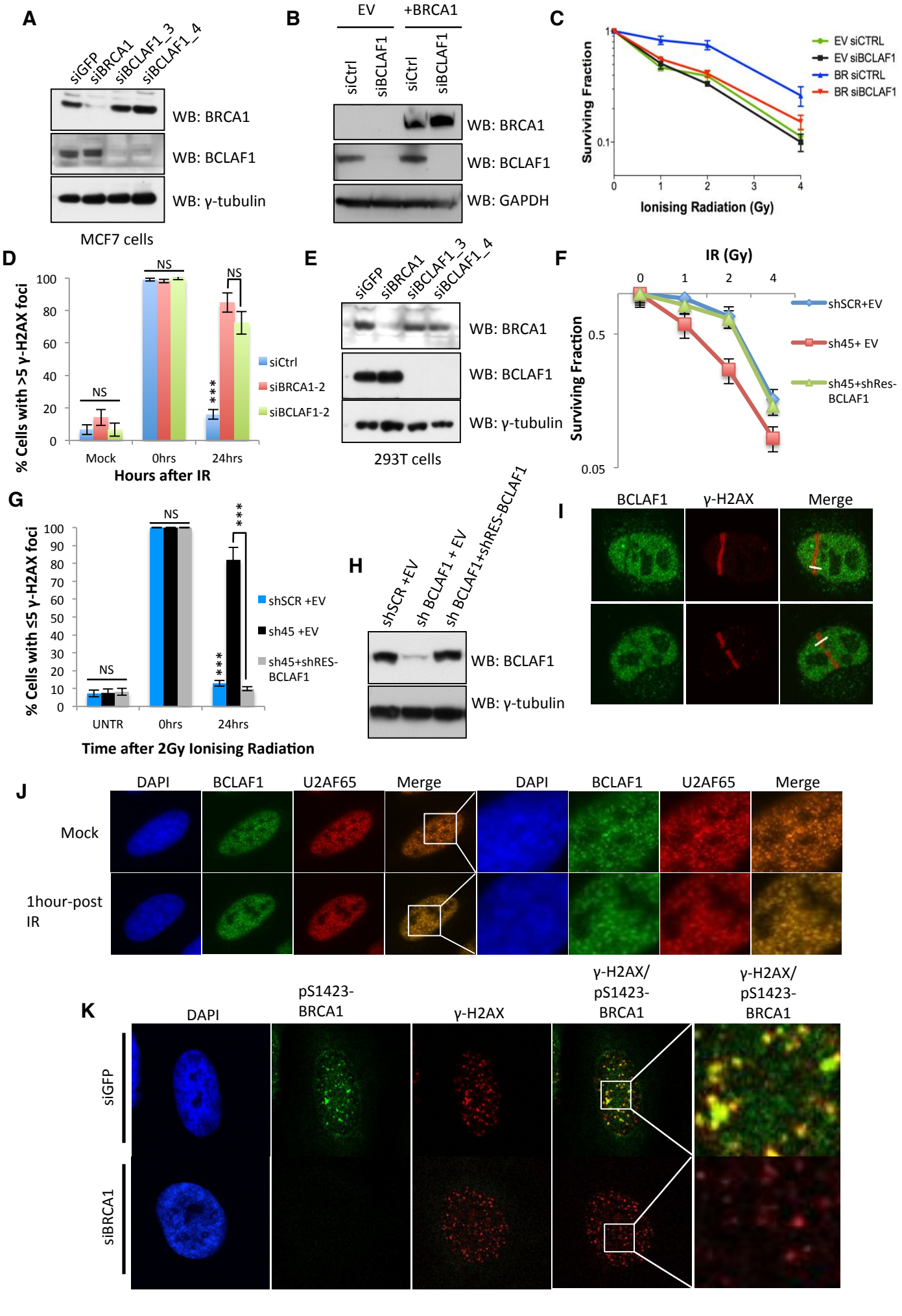
A
siGFP
siBRCA1
siBCLAF1_3
siBCLAF1_4
WB: BRCA1
WB: BCLAF1
WB: γ-tubulin
MCF7 cells
B
EV
+BRCA1
siCtrl
siBCLAF1
siCtrl
siBCLAF1
WB: BRCA1
WB: BCLAF1
WB: GAPDH
C
Surviving Fraction
Ionising Radiation (Gy)
EV siCTRL
EV siBCLAF1
BR siCTRL
BR siBCLAF1
D
% Cells with >5 γ-H2AX foci
Hours after IR
Mock
0hrs
24hrs
NS
***
siCtrl
siBRCA1-2
siBCLAF1-2
E
siGFP
siBRCA1
siBCLAF1_3
siBCLAF1_4
WB: BRCA1
WB: BCLAF1
WB: γ-tubulin
293T cells
F
IR (Gy)
Surviving Fraction
shSCR+EV
sh45+ EV
sh45+shRes-BCLAF1
G
% Cells with ≤5 γ-H2AX foci
Time after 2Gy Ionising Radiation
UNTR
0hrs
24hrs
shSCR +EV
sh45 +EV
sh45+shRES-BCLAF1
H
shSCR +EV
sh BCLAF1 + EV
sh BCLAF1+shRES-BCLAF1
WB: BCLAF1
WB: γ-tubulin
I
BCLAF1
γ-H2AX
Merge
J
DAPI
BCLAF1
U2AF65
Merge
Mock
1hour-post IR
K
DAPI
pS1423-BRCA1
γ-H2AX
γ-H2AX/ pS1423-BRCA1
siGFP
siBRCA1

Figure S2. BCLAF1 depletion induces sensitivity to DNA damage and defective DNA repair, related to Figure 2.

A. Representative western blots demonstrating BRCA1 and BCLAF1 depletion in MCF7 used for clonogenic survival assays **B.** Representative western blots demonstrating BRCA1 expression and BCLAF1 depletion in MDA-MB-436 (BRCA1 -/-) cells stably transfected with pcDNA 3.1 empty vector (EV) or pcDNA 3.1-BRCA1 and transiently transfected with control or BCLAF1 targeted siRNAs. **C.** Clonogenic survival assays performed in MDA-MB-436 described above (B). Mean surviving fraction of three independent experiments is plotted +/- SEM. **D.** Repeat of Figure 2D using independent BRCA1 and BCLAF1 siRNAs. Representative western blot demonstrating depletion of BRCA1 and BCLAF1 with these siRNAs is shown in figure S3C. Significant differences in the fraction of cells containing ≥5 γ-H2AX foci were assessed using a students two-tailed t-test and are indicated by * = $P < 0.05$; ** = $P < 0.01$; *** = $P < 0.001$. **E**. Representative western blots demonstrating BRCA1 and BCLAF1 depletion in 293T cells used for DNA repair assays. **F.** Clonogenic survival assays performed in 293T cells stably transfected with a scrambled control shRNA (shSCR) or a BCLAF1 targeted shRNA (shBCLAF1) which had been co-transfected with either an empty expression vector (EV) or the same expression vector containing an shRNA resistant BCLAF1 cDNA (shRES-BCLAF1). Mean surviving fraction of three independent experiments is plotted +/- SEM. **G.** Repair of γ-H2AX marked DNA damage in 293T cells stably transfected with a scrambled control shRNA (shSCR) or a BCLAF1 targeted shRNA (shBCLAF1) which had been co-transfected with either an empty expression vector (EV) or the same expression vector containing an shRNA resistant BCLAF1 cDNA (shRES-BCLAF1). Cells were either untreated or treated with 2 Gy IR and fixed 0 and 24 hours after treatment. Mean fraction of cells containing ≥5 γ-H2AX foci from three independent experiments (≥200 cells were scored/experiment) is plotted +/- SEM. Significant differences in the fraction of cells containing ≥5 γ-H2AX foci were assessed using a students two-tailed t-test and are indicated by * = $P < 0.05$; ** = $P < 0.01$; *** = $P < 0.001$. **H.** Representative western blot demonstrating efficient shRNA mediated depletion of BCLAF1 and rescue of BCLAF1 expression with shRES-BCLAF1 expression in cells used for clonogenic survival and DNA repair assays shown in Figures S2 H-I. **I.** Localised tracks of DNA damage were induced in HeLa cells by laser micro-irradiation and cells stained for γ-H2AX and BCLAF1. Cells were then imaged using confocal microscopy indicating that BCLAF1 is excluded from γ-H2AX marked DNA break sites. **J.** Immunofluorescent staining of BCLAF1 and U2AF65 in mock irradiated or irradiated (2Gy whole field IR) U2OS cells fixed 1 hour after irradiation. Panels on right show magnified images of region highlighted by box. **K.** Representative immunofluorescent staining of chromatin bound γ-H2AX & pS1423-BRCA1 (using phospho-specific antibodies) 1 hour following treatment with ionising radiation (2Gy). Non-chromatin bound proteins were extracted by pre-treatment of control (siGFP) and BRCA1 depleted (siBRCA1) cells with mild detergent extraction buffer prior to fixation (see materials and methods). Cells were then stained with pS1423-BRCA1 and γ-H2AX antibodies. Cells were then imaged using a Leica SP5 confocal microscope. Panels on the right show magnified images of the merged γ-H2AX/pS1423-BRCA1 staining within regions highlighted by box. This demonstrates that pS1423-BRCA1 forms at DNA break sites (demonstrated by co-localisation with γ-H2AX), but also displays additional nuclear staining suggesting that it may also bind at other regions of chromatin. Loss of both γ-H2AX associated and additional chromatin bound pS1423-BRCA1 staining in siBRCA1 transfected cells demonstrates the specificity of this staining. Similar results were seen in the majority of cells in each field and in repeat experiments.

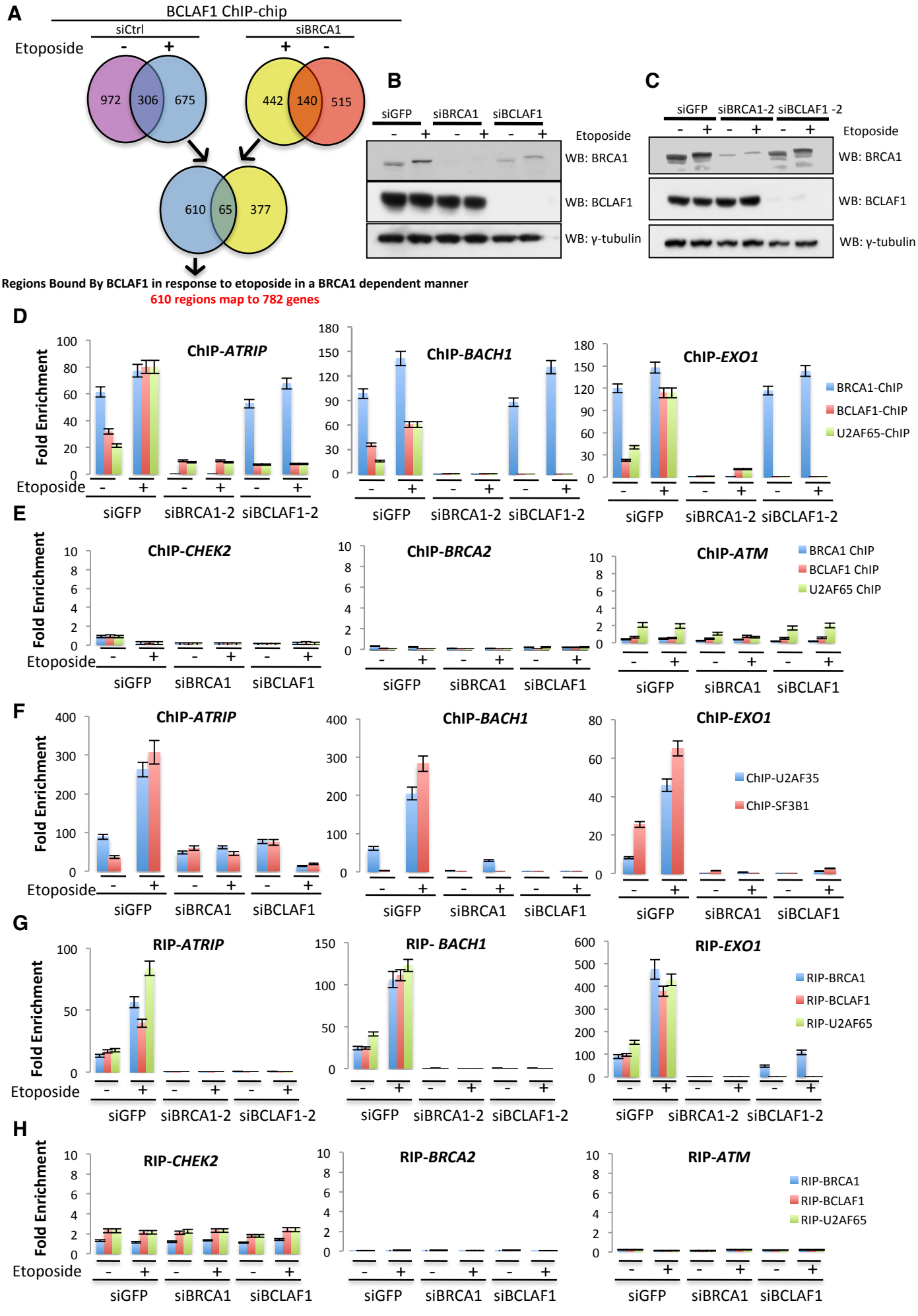
A
BCLAF1 ChIP-chip
siCtrl
siBRCA1
Etoposide
972
306
675
442
140
515
610
65
377
Regions Bound By BCLAF1 in response to etoposide in a BRCA1 dependent manner
610 regions map to 782 genes
B
siGFP
siBRCA1
siBCLAF1
Etoposide
WB: BRCA1
WB: BCLAF1
WB: γ-tubulin
C
siGFP
siBRCA1-2
siBCLAF1 -2
Etoposide
WB: BRCA1
WB: BCLAF1
WB: γ-tubulin
D
ChIP-ATRIP
ChIP-BACH1
ChIP-EXO1
Fold Enrichment
BRCA1-ChIP
BCLAF1-ChIP
U2AF65-ChIP
Etoposide
siGFP
siBRCA1-2
siBCLAF1-2
E
ChIP-CHEK2
ChIP-BRCA2
ChIP-ATM
Fold Enrichment
BRCA1 ChIP
BCLAF1 ChIP
U2AF65 ChIP
Etoposide
siGFP
siBRCA1
siBCLAF1
F
ChIP-ATRIP
ChIP-BACH1
ChIP-EXO1
Fold Enrichment
ChIP-U2AF35
ChIP-SF3B1
Etoposide
siGFP
siBRCA1
siBCLAF1
G
RIP-ATRIP
RIP- BACH1
RIP-EXO1
Fold Enrichment
RIP-BRCA1
RIP-BCLAF1
RIP-U2AF65
Etoposide
siGFP
siBRCA1-2
siBCLAF1-2
H
RIP-CHEK2
RIP-BRCA2
RIP-ATM
Fold Enrichment
RIP-BRCA1
RIP-BCLAF1
RIP-U2AF65
Etoposide
siGFP
siBRCA1
siBCLAF1

Figure S3. Recruitment of BRCA1-mRNA splicing complex proteins to the ATRIP, BACH1 and EXO1 promoters, related to Figure 3.

A. BCLAF1 Chromatin Immunoprecipitation array hybridisation (ChIP-chip) was performed from etoposide treated (1μM, 16hrs) 293T cells transfected with control or BRCA1 targeted siRNAs. ChIPs were performed in triplicate. BCLAF1 bound regions were identified using Niblescan and MA2C. Regions bound in at least 2 of 3 triplicate arrays were identified. Lists of regions bound by BCLAF1 in response to etoposide were generated for siCtrl and siBRCA1 cells. These lists were then compared to identify regions bound by BCLAF1 in the presence of BRCA1 (i.e. in control cells only). This generated a list of 610 regions that were bound by BCLAF1 in response to etoposide in a BRCA1 dependent manner. Mapping of these regions to genes surrounding the binding regions or within 10kb upstream of the bound region generated a list of 782 genes that are potentially regulated by BCLAF1 in response to etoposide in a BRCA1 dependent manner. **B-C.** Representative western blots demonstrating depletion of BRCA1 and BCLAF1 with different siRNAs in cells used for DNA repair, ChIP and RIP assays. **D.** BRCA1, BCLAF1 and U2AF65 ChIP-qRT-PCRs examining binding to the *ATRIP, BACH1* and *EXO1* promoters in untreated and etoposide treated, control cells (siGFP) and cells depleted of BRCA1 and BCLAF1 using additional siRNAs (siBRCA1-2 and siBCLAF1-2). Graphs represent the mean fold enrichment from three independent experiments +/- SEM. **E.** BRCA1, BCLAF1 and U2AF65 ChIP-qRT-PCRs examining binding to the *CHEK2, BRCA2* and *ATM* promoters (DDR genes not identified in the BCLAF1 ChIP-chip) in untreated and etoposide treated, control cells (siGFP) and cells depleted of BRCA1 and BCLAF1 (siBRCA1 and siBCLAF1). Graphs represent the mean fold enrichment from three independent experiments +/- SEM. Similar results were seen in cells depleted of BRCA1 and BCLAF1 using independent siRNAs (data not shown). **F.** U2AF35 AND SF3B1 ChIP-qRT-PCRs examining binding to the *ATRIP, BACH1* and *EXO1* promoters in untreated and etoposide treated, control cells (siGFP) and cells depleted of BRCA1 and BCLAF1. Graphs represent the mean fold enrichment from three independent experiments +/- SEM. **G.** BRCA1, BCLAF1 and U2AF65 RIP-qRT-PCRs examining binding to *ATRIP, BACH1* and *EXO1* mRNAs in untreated and etoposide treated, control cells (siGFP) and cells depleted of BRCA1 and BCLAF1 using additional siRNAs (siBRCA1-2 and siBCLAF1-2). Graphs represent the mean fold enrichment from three independent experiments +/- SEM. All RNA was DNAse treated prior to cDNA synthesis and a reverse transcriptase negative (RT-ve) control sample was generated and subjected to the same qRT-PCR reaction to ensure no genomic DNA contamination (Data not shown). **H.** BRCA1, BCLAF1 and U2AF65 RIP-qRT-PCRs examining binding to *CHEK2, BRCA2* and *ATM* mRNAs (DDR genes not identified in the BCLAF1 ChIP-chip) in untreated and etoposide treated, control cells (siGFP) and cells depleted of BRCA1 and BCLAF1 (siBRCA1 and siBCLAF1). Graphs represent the mean fold enrichment from three independent experiments +/- SEM. Similar results were seen in cells depleted of BRCA1 and BCLAF1 using independent siRNAs (data not shown). All RNA was DNAse treated prior to cDNA synthesis and an RT-ve control sample was generated and subjected to the same qRT-PCR reaction to ensure no genomic DNA contamination (Data not shown).

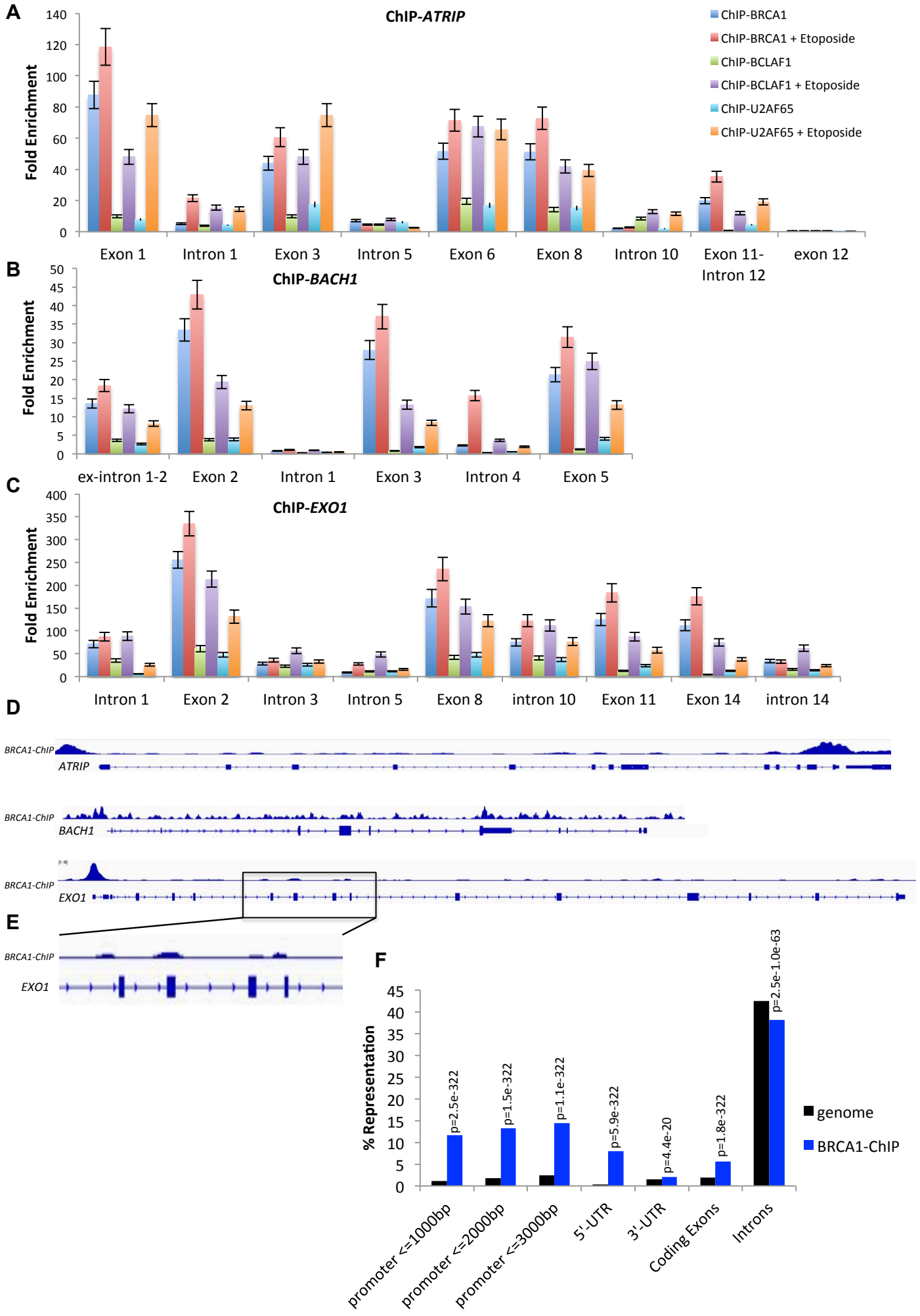
A
ChIP-ATRIP
Fold Enrichment
ChIP-BRCA1
ChIP-BRCA1 + Etoposide
ChIP-BCLAF1
ChIP-BCLAF1 + Etoposide
ChIP-U2AF65
ChIP-U2AF65 + Etoposide
Exon 1
Intron 1
Exon 3
Intron 5
Exon 6
Exon 8
Intron 10
Exon 11-Intron 12
exon 12
B
ChIP-BACH1
Fold Enrichment
ex-intron 1-2
Exon 2
Intron 1
Exon 3
Intron 4
Exon 5
C
ChIP-EXO1
Fold Enrichment
Intron 1
Exon 2
Intron 3
Intron 5
Exon 8
intron 10
Exon 11
Exon 14
intron 14
D
BRCA1-ChIP
ATRIP
BRCA1-ChIP
BACH1
BRCA1-ChIP
EXO1
E
BRCA1-ChIP
EXO1
F
% Representation
p=2.5e-322
p=1.5e-322
p=1.1e-322
p=5.9e-322
p=4.4e-20
p=1.8e-322
p=2.5e-1.0e-63
genome
BRCA1-ChIP
promoter <=1000bp
promoter <=2000bp
promoter <=3000bp
5'-UTR
3'-UTR
Coding Exons
Introns

Figure S4. BRCA1, BCLAF1 and U2AF65 bind throughout *ATRIP, BACH1* and *EXO1* genes exonic regions, related to Figure 3.

A-C. BRCA1, BCLAF1 and U2AF65 ChIP-qRT-PCRs demonstrating constitutive binding of BRCA1 to the indicated regions within *ATRIP, BACH1* and *EXO1* in the presence and absence of DNA damage (Etoposide). The ChIPs also demonstrate that BCLAF1 and U2AF65 are only recruited to these genetic regions following DNA damage in a BRCA1 and BCLAF1 dependent manner respectively. These assays also demonstrate that BRCA1, BCLAF1 and U2AF65 bind more strongly to exons and exon-intron boundary regions with limited binding within introns. Additionally, reduced binding of all three proteins is observed with progression toward the 3` end of each gene which is consistent with reduced transcript tethering concurrent with transcriptional termination. These chromatin binding characteristics are consistent with many other mRNA splicing proteins. Graphs represent the mean fold enrichment quantified from three independent experiments +/- SEM. **D.** BRCA1 binding profile generated from publically available BRCA1-ChIP-seq data demonstrating BRCA1 binding at the promoters as well as at exonic regions of the ATRIP, BACH1 and EXO1 genes. **E** Magnified region of BRCA1 binding within the EXO1 gene demonstrating BRCA1 binding at EXO1 exonic regions. **F.** Genome wide analysis carried out using the Cis-Regulatory Element Annotation System (CEAS) examining statistical enrichment of BRCA1 binding peaks relative to a range of genomic features. This demonstrates that, on a genome wide level, BRCA1 binding peaks are enriched within gene promoters, 5'-UTRs and exons. In contrast, BRCA1 binding peaks are significantly underrepresented within genetic introns.

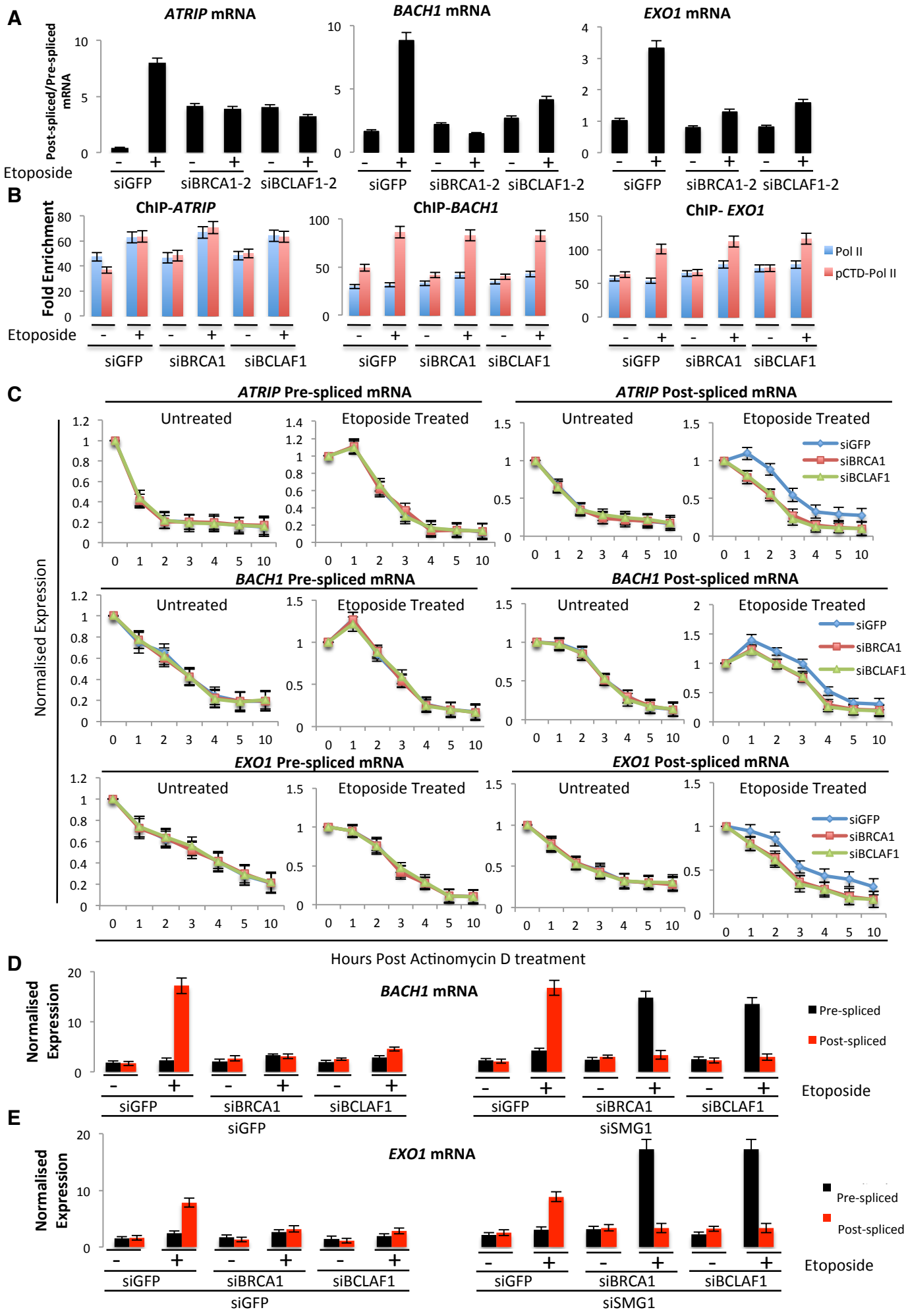
A
ATRIP mRNA
BACH1 mRNA
EXO1 mRNA
Post-spliced/Pre-spliced mRNA
Etoposide
siGFP
siBRCA1-2
siBCLAF1-2
B
ChIP-ATRIP
ChIP-BACH1
ChIP- EXO1
Fold Enrichment
Pol II
pCTD-Pol II
siBRCA1
siBCLAF1
C
ATRIP Pre-spliced mRNA
ATRIP Post-spliced mRNA
BACH1 Pre-spliced mRNA
BACH1 Post-spliced mRNA
EXO1 Pre-spliced mRNA
EXO1 Post-spliced mRNA
Untreated
Etoposide Treated
Normalised Expression
D
Hours Post Actinomycin D treatment
BACH1 mRNA
Normalised Expression
Pre-spliced
Post-spliced
siSMG1
E
EXO1 mRNA

Figure S5. BRCA1/BCLAF1 regulates DNA damage induced *ATRIP, BACH1 and EXO1* splicing, related to Figure 4.

A. Repeat of figure 4a with additional siRNAs and exon-exon and exon-intron primer sets**.** Ratio of post-spliced to pre-spliced *ATRIP, BACH1* and *EXO1* mRNA in control (siGFP) and BRCA1 or BCLAF1 depleted cells mock treated or treated with etoposide. mRNA levels were assessed by qRT-PCR using exon 1-exon 2 (post-spliced-*ATRIP*) and exon 1-intron 1 (pre-spliced-*ATRIP*), exon 3-exon 4 (post-spliced-*BACH1*) and exon 3-intron 3 (pre-spliced- *BACH1*) and exon 6-exon 7 (post-spliced-*EXO1*) and exon 6-intron 6 (pre-spliced- *EXO1*), qRT-PCR primers and normalised to *ACTB* mRNA. Graphs represent the mean ratios of post-spliced/pre-spliced mRNA from three independent experiments +/- SEM. All RNA was DNAse treated prior to cDNA synthesis and an RT-ve control sample was generated and subjected to the same qRT-PCR reaction to ensure no genomic DNA contamination (Data not shown). Significance of changes in splicing ratios following etoposide treatment was assessed using students two-tailed t-test with significant changes indicated by * = $P < 0.05$; ** = $P < 0.01$; *** = $P < 0.001$. **B.** ChIP-qRT-PCR assays performed with antibodies against the major RNA Pol II subunit POLR2H (Pol II) or actively transcribing RNA Pol II (pCTD-Pol II) demonstrating levels of total RNA Pol II and active RNA Pol II on the *ATRIP, BACH1* and *EXO1* promoter regions, in control (siCtrl) and BRCA1 or BCLAF1 depleted cells either mock treated or treated with etoposide. Graphs represent the mean fold enrichment quantified from three independent experiments +/- SEM. **C.** qRT-PCR analysis of pre-spliced and post-spliced *ATRIP, BACH1* and *EXO1* mRNA levels following inhibition of transcription with Actinomycin D treatment in unperturbed or etoposide treated (1µM, 16hrs) cells transfected with control (siCtrl), BRCA1 and BCLAF1 siRNAs. Pre-spliced and post-spliced mRNA levels were assessed by qRT-PCR using the same primer sets as described in (A). Data points represent the mean normalised expression of three independent experiments +/- SEM. **D-E.** Normalised expression levels of post-spliced and pre-spliced *BACH1* and *EXO1* mRNA in control (siGFP) and BRCA1 or BCLAF1 depleted cells transfected with control siRNA (siCtrl) or depleted of SMG1 a key regulator of the non-sense mediated decay pathway. Cells were mock treated or treated with Etoposide and mRNA levels were assessed as described in (A). Graphs represent the mean normalised expression from three independent experiments +/- SEM. Depletion of BRCA1, BCLAF1 and SMG1 was assessed by qRT-PCR and determined to be >90%.

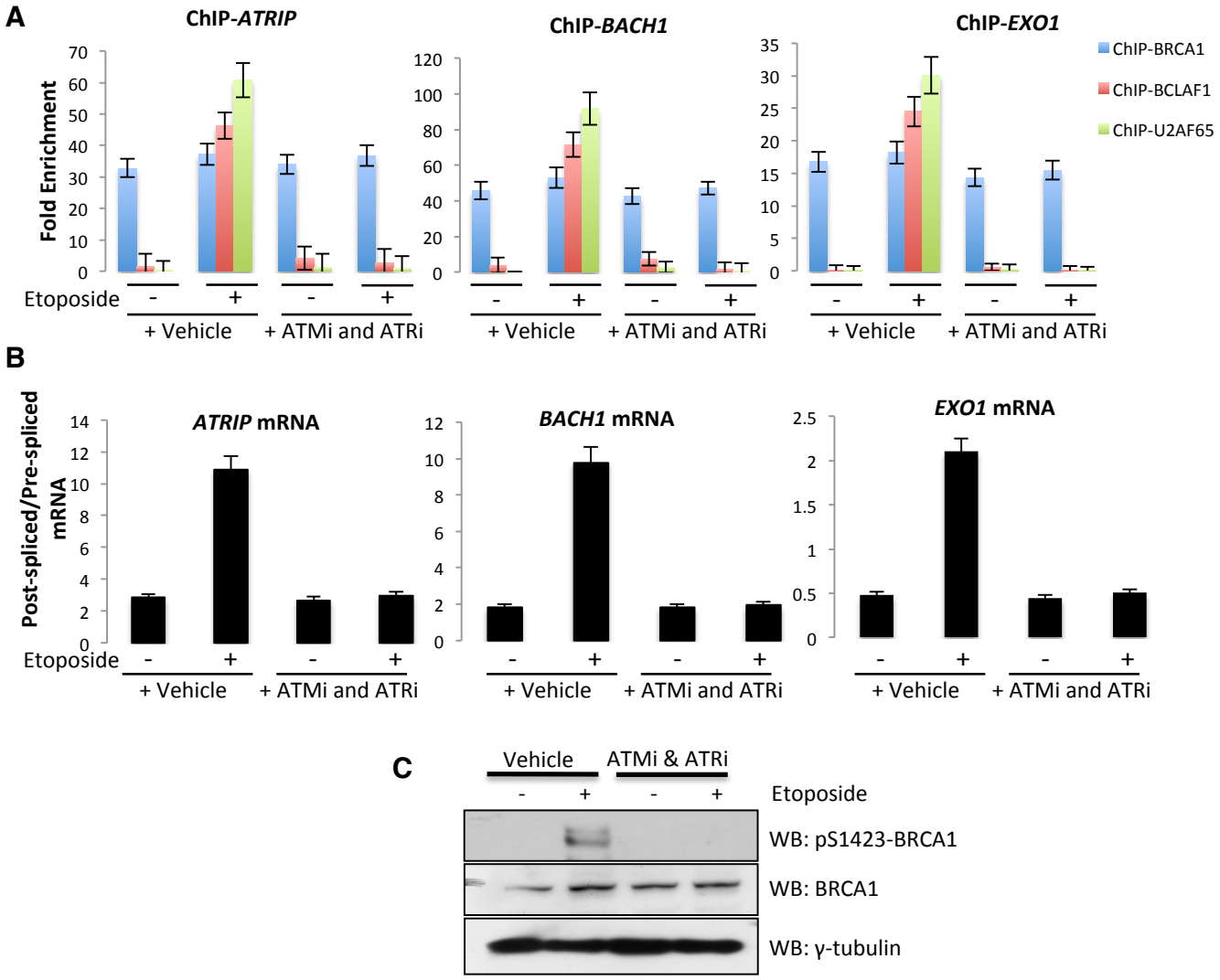

Figure S6. Inhibition of ATM/ATR blocks DNA damage induced *ATRIP, BACH1* and *EXO1* splicing through inhibition of BCLAF1 and U2AF65 recruitment, related to Figure 5.

A. BRCA1, BCLAF1 and U2AF65 ChIP-qRT-PCRs examining binding to the *ATRIP, BACH1* and *EXO1* promoters in untreated and etoposide treated 293T cells pre-treated with vehicle (DMSO) or ATM and ATR inhibitors. Graphs represent the mean fold enrichment from three independent experiments +/- SEM. **B.** Ratio of post-spliced to pre-spliced *ATRIP, BACH1* and *EXO1* mRNAs determined by qRT-PCR (as described in figure 5A-G) in untreated and etoposide treated 293T cells pre-treated with vehicle (DMSO) or ATM and ATR inhibitors. Graphs represent the mean fold enrichment from three independent experiments +/- SEM. **C.** Representative western blot demonstrating that inhibition of ATM/ATR blocks BRCA1-S1423 phosphorylation following etoposide treatment.

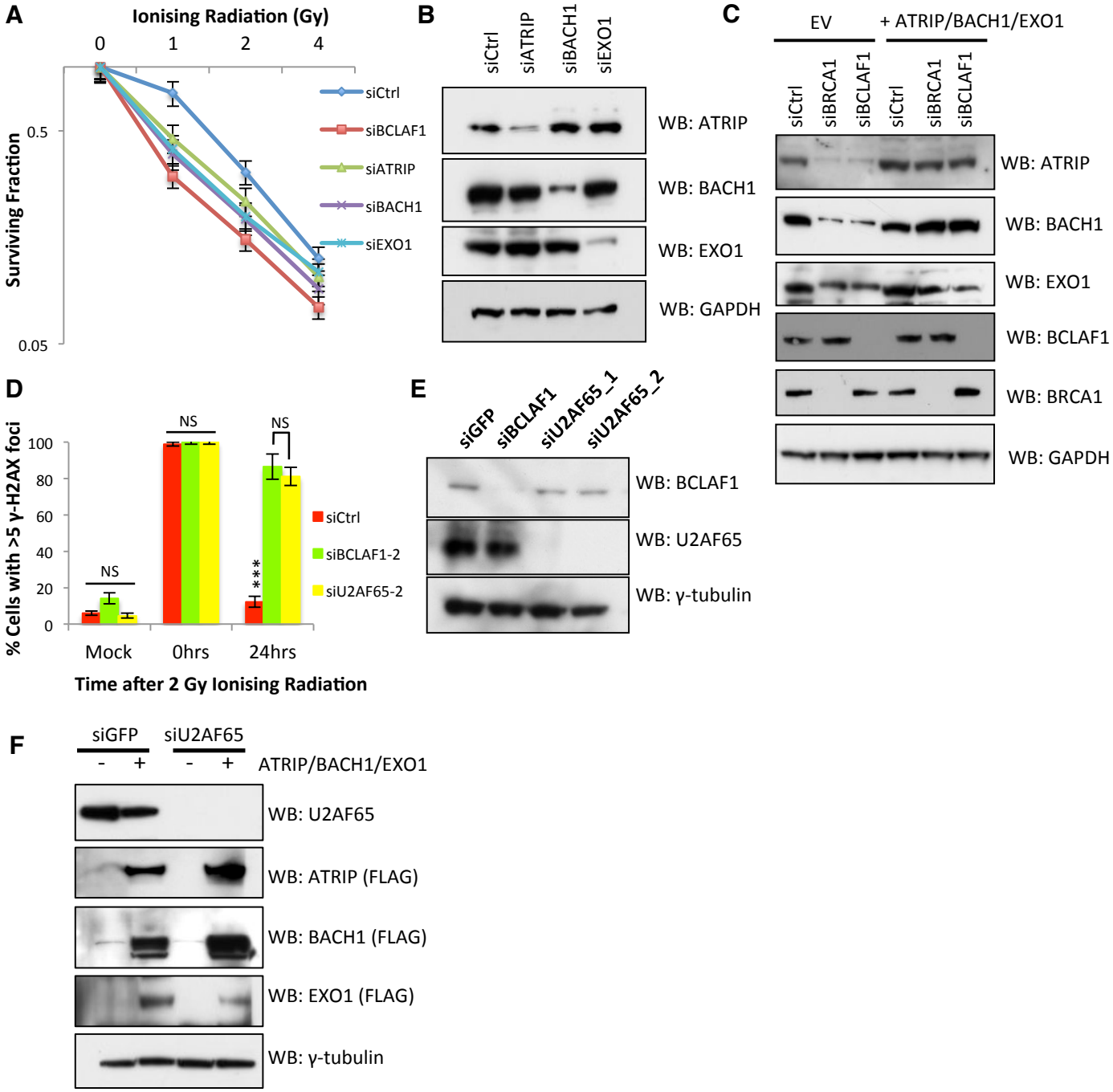

Figure S7. ATRIP, BACH1 and EXO1 are required for BRCA1, BCLAF1 and U2AF65 mediated resistance to DNA damage, related to Figure 7.

A. Clonogenic survival assays performed in control (siCtrl) cells and cells transfected with titrated concentrations of ATRIP, BACH1 and EXO1 siRNAs demonstrating that reduction but not complete loss of any of these proteins to similar levels as that observed in BRCA1 or BCLAF1 depleted cells post-DNA damage, induces sensitivity to ionising radiation (IR). Mean surviving fraction of three independent experiments is plotted +/- SEM. **B.** Representative western blots demonstrating partial knockdown of ATRIP, BACH1 and EXO1 in cells used for clonogenic survival assays in (A). **C.** Representative western blots demonstrating ectopic expression of ATRIP, BACH1 and EXO1 in control (siCtrl) and BRCA1 or BCLAF1 depleted 293T cells transfected with empty vector (EV) or a combination of ATRIP, BACH1 and EXO1 expression vectors. All of these cells have been treated with Etoposide (1μM 16 hrs). These cells were used for clonogenic survival assays shown in figure 6B. **D.** Repeat of Figures 6E using different BCLAF1 and U2AF65 siRNAs. **E.** Representative western blot demonstrating depletion of BCLAF1 and U2AF65 in cells used for clonogenic survival and DNA repair assays. **F.** Representative western blot showing ectopic expression of FLAG tagged ATRIP, BACH1 and EXO1 in U2AF65 depleted cells used for clonogenic survival assays shown in figure 6F.

Supplemental Experimental Procedures

Cell-lines

293T cells were obtained from the Cancer Research UK cell Repository (London Research Institute, London) and MCF7 cells were obtained from the European Collection of Cell Vultures (ECACC), Wiltshire, UK. Both cell lines were verified by STR profiling (ATCC-LGC Standards, Middlesex ,UK). MDA-MB-436 cells were a kind gift from Prof. Nicola Curtin (Newcastle University). BRCA1 All cell lines were maintained in DMEM media (Sigma-Aldrich) containing 10% Foetal Calf Serum.

Peptide Pull-down Assays

Peptide Pull-down Assays were carried out as previously described (Stucki et al., 2005) using the following biotinylated peptides BRCA1-S1423: AVLEGHG**S**GPSNSYP, BRCA1-phospho-S1423: AVLEGHG**pS**GPSNSYP (Genscript).

siRNAs

siRNAs with the following sequences were obtained from QIAGEN; siBRCA1: 5'-CAG GAA ATG GCT GAA CTA GAA-3`, siBRCA1_2: 5'- ACC ATA CAG CTT CAT AAA TAA -3' siBCLAF1_2: 5`CUA GAU UAC UUC AGU GAU ATT-3` 5` siBCLAF1_3: 5`GAA UCU GGA UGC ACG AGA ATT-3`, siBCLAF_4 5`-UAG UAG AGA UCG UAU GUA UTT-3` (siBCLAF1 contains 50% siBCLAF1_3 and 50% siBCLAF_4 siRNAs). siU2AF65_1: 5`-GAG GAG AUA AUC UCG GAA ATT-3`, siU2AF65_2: 5`GCU UAC CCA ACU ACC UGA ATT3`, U2AF65_3: 5'-GUG AGU ACG UGG ACA UCA ATT-3` (siU2AF65 contains 50% siU2AF65_1 and 50% siU2AF65_2 siRNAs). siRNA Oligos were delivered to a final concentration of 10nM by reverse transfection using RNAiMax (Invitrogen) according to manufacturer's instructions.

Plasmids

The Flag-tagged BRCA1 construct Fl4-BRCA1 was a kind gift from Professor Richard Baer, Columbia University, New York, USA. Myc-DDK tagged ATRIP (RC223562), BACH1 (RC224085), and EXO1 (RC200547) plasmids were

purchased from Origene. Plasmids were transfected with Genejuice (Merck) as per the manufacturers instructions.

Site Directed Mutagenesis

The Quick Change Site Directed Mutagenesis kit (Stratagene) was used, as per the manufacturers instructions to introduce the S1423A substitution within the Fl4-BRCA1 construct using the following primers: BRCA1_S1423A_Fwd 5'-GAA CAG CAT GGG **GCC** CAG CCT TCT AAC-3' and BRCA1_S1423A_Rev 5'-GTT AGA AGG CTG **GGC** CCC ATG CTG TTC-3'.

qRT-PCR and splicing analysis

2 μg of RNA was DNAse (Invitrogen) treated as per the manufacturers instructions. 1 μg of DNAse treated RNA was then used for cDNA synthesis using the Transcriptor High Fidelity cDNA Synthesis Kit (Roche Applied Science) according to the manufacturer's instructions. The remaining 1 μg of RNA was used for an identical cDNA synthesis reaction containing no reverse transcriptase (RT-ve). qRT-PCR was performed using primers specific to each transcript, or to ACTB mRNA on both RT positive and RT negative generated cDNA. All reciprocal qRT-PCR reactions performed on RT –ve cDNA were assessed for the absence of any cDNA amplification indicating no genomic DNA contamination prior to further analysis of data. All qRT-PCR reactions were carried out on a ROCHE LightCycler 480 as using SYBR Green 480 I Master Mix (ROCHE) as per the manufacturers instructions. mRNA concentration levels were then assessed using the ROCHE Relative Quantification algorithm utilising in-run standard curve qRT-PCR data generated for each primer set from a serially diluted RNA standard.

For quantitative splicing analysis, introns/exons were chosen for assessment in splicing analysis based on their suitability for optimal qRT-PCR primer design. Primers spanning exon-exon boundaries (post-spliced) and exon-intron boundaries (pre-spliced) were designed using the ROCHE universal probe library and manually inputting exon-exon and exon-intron flanking sequences. Using these primers (listed below) levels of pre-spliced and post-spliced mRNAs

were assessed as above and normalised to ACTB expression levels within the same samples. Ratio's of post-spliced to pre-spliced mRNAs were then calculated by dividing the normalised levels of each transcript.

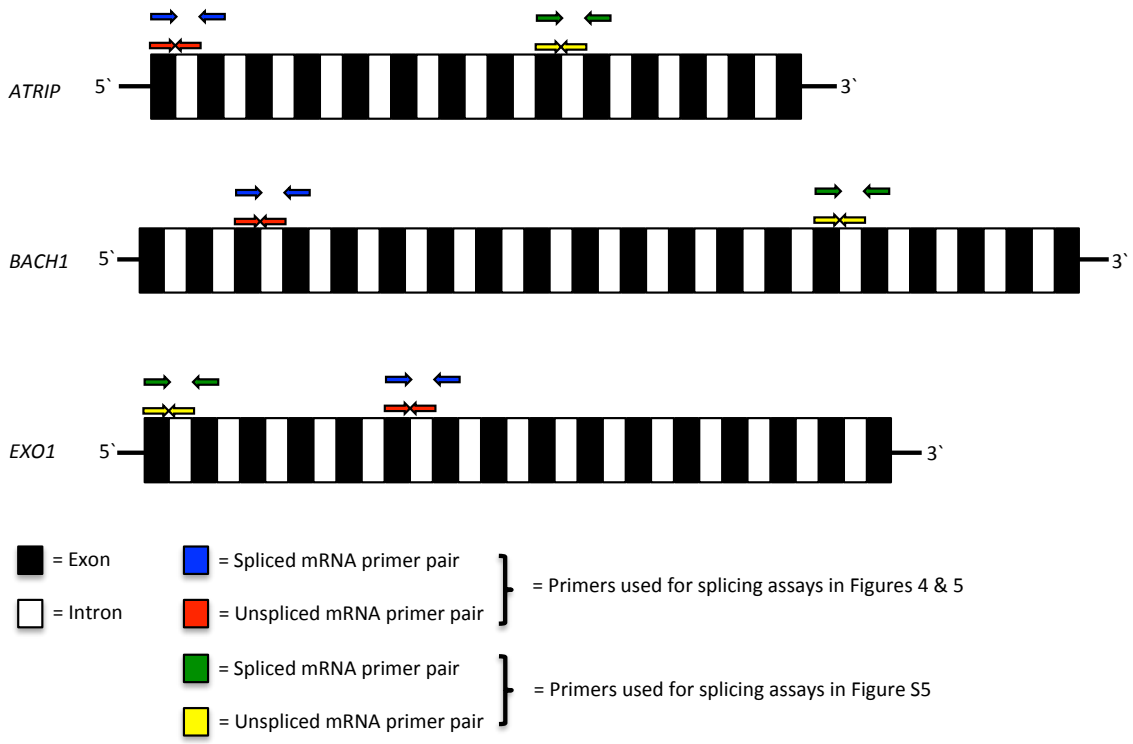

Primer sequences used are as follows:

<u>Splicing Analysis:</u>

Exo1_(Int7)_Unspliced_Fwd_1: ccaaatgtattttattgtattttgcag,

Exo1_(Int7)_Unspliced_Rev_1: gatgttatctctgactggggaca,

Exo1_(Int7)_Spliced_Fwd_1: tgagctctggaaaaactttgg,

Exo1_(Int7)_Spliced_Rev_1: ctggggacaggggtttct,

BACH1_(Int4)_Pre-spliced_Fwd_1: ttaggaaacctcccaatcctg,

BACH1_ (Int4)_Pre-spliced_Rev_1: tgctggtttccctaaaaatga,

BACH1_ (Int4)_Spliced_Fwd_1: aatggcacttcatcaacttgtc,

BACH1_ (Int4)_Spliced_Rev_1: tggatgcctgtttcttagca,

ATRIP_(Int1)_Unspliced_Fwd_1: gcatggggacttcactgc,

ATRIP_(Int1)_Unspliced_Rev_1: ggagcactcactggacacg,

ATRIP_(Int1)_Spliced_Fwd_1: gcatggggacttcactgc,

ATRIP_(Int1)_Spliced_Rev_1: gaccttatgatcactggacacg,

Exo1_(Int1)_Spliced_Fwd: tttctccaaccgcaatcg

Exo1_(Int1)_Spliced_Rev: gacgacacgtttccttaggc

Exo1_(Int1)_Unspliced_Fwd: tttctccaaccgcaatcg

Exo1_(Int1)_Unspliced_Rev: tgttgggttgggaagatcac

BACH1_(Int15)_Spliced_Fwd: tggagttggtgaagacagtca

BACH1_(Int15)_Spliced_Rev: ctaccaggagagctccatcttt

BACH1_(Int15)_Unspliced_Fwd: tggcataatctggagttggtg

BACH1_(Int15)_Unspliced_Rev: ttttcaccgaccatgaaataa

ATRIP_(Int9)_Spliced_Fwd: ctgtgatttcttgcccaggt

ATRIP_(Int9)_Spliced_Rev: gggagaggagctcaacagc

ATRIP_(Int9)_Unspliced_Fwd: ctgtgatttcttgcccaggt

ATRIP_(Int9)_Unspliced_Rev: ttccttggttctcccatttg

ACTB_RT_Fwd: ccaaccgcgagaagatga,

ACTB_RT_Rev: ccagaggcgtacagggatag

ChIP/RIP Analysis:

ATRIP_ChIP/RIP_Fwd: TTAGGCCACTTGGTTCTTGG

ATRIP_ChIP/RIP_Rev: GGGAGACAGTGGGCTTCATA

BACH1_ChIP/RIP_Fwd: GTTTGGGGAAGGAGTTTGCT

BACH1_ChIP/RIP_Rev: GACAATGAGGCAAACAAATCAA

EXO1_ChIP/RIP: Fwd GCACTGTGCACAATTCCTTC

EXO1_ChIP/RIP_Rev: AACCTCAAGTGTTGGGCAAG

Non-specific_Control_Region_Fwd: AAAGCACTGTGTTCTTAGCACCGCGGGT

Non-specific_Control_Region_Rev: CCCTAGGGCTTGATGGGAACGGGAAACCTT

(Used for ChIP Assays Only)

ACTB_Control_Region_Fwd: CCGAAAGTTGCCTTTTATGG

ACTB_Control_Region_Rev: CAAAGGCGAGGCTCTGTG

(Used for RIP Assays)

Alternative splicing Analysis

ATRIP_E2_Fwd: TCCTTCAGGGAAAAACAGAGA
ATRIP_E12_Rev: ACGCAGTGCATCATGAAGAG
BACH1_E1_Fwd: CAATTGGTGGGGTGAAGATT
BACH1_E20_Rev: CAGGTGTTGCCTTCGGTATT
EXO1_E3_Fwd: GCTTCAGAACCCATCCATGT
EXO1_E14_Rev: TATCCTCTTCCGCTTCTGGA

Semi-quantitative PCR analysis of Intronic Regions

2 µg of RNA was DNAse (Invitrogen) treated as per the manufacturers instructions. 1 µg of DNAse treated RNA was then used for cDNA synthesis using the Transcriptor High Fidelity cDNA Synthesis Kit (Roche Applied Science) according to the manufacturer's instructions. The remaining 1 µg of RNA was used for an identical cDNA synthesis reaction containing no reverse transcriptase (RT-ve). Semi-quantitative PCR was carried out using Megamix-Gold (Micozone) as per the manufacturers instructions over 50 PCR cycles. A reciprocal Semi-quantitative PCR was carried out on all RT –ve cDNAs and assessed by agarose gel electrophoresis to assure no genomic DNA contamination. Semi-quantitative PCR derived amplicons were assessed by Agarose gel electrophoresis and imaged using a UV gel documentation system. Primer sequences used are as follows:

ATRIP_Intron_1_Fwd: ctaggagggtgaggcacaag
ATRIP_Intron_1_Rev: gagagcaaagcagggaaaga
ATRIP_Intron_10_Fwd: acagatgcaatgcagacagg
ATRIP_Intron_10_Rev: caagaagtggtgtgggacct
BACH1_Intron_1_Fwd: ggtacattctgccctggcta
BACH1_Intron_1_Rev: caggatgggctttggagtaa
BACH1_Intron_18_Fwd: tattgggaacaatgctgcaa
BACH1_Intron_18_Rev: aaactggaacccttgtgtgc
EXO1_Intron_2_Fwd: gctttcagagaggctgatgg
EXO1_Intron_2_Rev: aagggtcaacgtgcaaattc
EXO1_Intron_14_Fwd: gagtgagagcccacttcctg
EXO1_Intron_14_Rev: tggaatttgctgtggactga

CHEK2_Intron_3_Fwd: agaagtgcttaaggccacga

CHEK2_Intron_3_Rev: gcaaaatgcaacacccttttt

CHEK2_Intron_3_Fwd: agaagtgcttaaggccacga

CHEK2_Intron_3_Rev: gcaaaatgcaacacccttttt

ATM_Intron_6_Fwd: gcgtggccaacattttaagt

ATM_Intron_6_Rev: ccagattcctccctagcaca

Clonogenic Survival Assays

293T or MCF7 cells were transfected with siRNAs and incubated for 62 hrs. Cells were then seeded as single cells at various densities. 10 hours later cells were mock treated or exposed to IR or medium containing Etoposide (Sigma-Aldrich). After 7-14 days cells were fixed, stained with crystal violet and colonies counted. Surviving fraction for each treatment/dose was calculated by normalising to plating efficiency for each siRNA treatment.

Ionising Radiation (IR)

Irradiations (IR) were carried out using an X-RAD 225 X-ray generator (Precision X-ray Inc. Branford, CT, USA) at a dose rate of 0.591 $Gy.min^{-1}$.

Co- Immunoprecipitations

2µg of primary antibody (BRCA1 (Ab1, Millipore) or BCLAF1 (BTF-608A, Bethyl Laboratories)) was coupled to anti-mouse or anti-rabbit Dynabeads (Invitrogen) respectively and added to 2mg of pre-cleared 293T or MCF7 whole cell lysate (ELB Lysis Buffer: 250mM NaCl, 5mM EDTA, 50mM HEPES, 0.1% v/v NP40). Immunoprecipitations were carried out overnight at $4^{o}C$ followed by 6 washes with ELB Buffer. Immunoprecipitated proteins were then re-suspended in 2x LDS loading buffer (Invitrogen).

Western Blotting

Whole cell extracts were prepared by lysing cells in 2 volumes of ELB buffer (250mM NaCl, 5mM EDTA, 50mM HEPES, 0.1% v/v NP40). 60µg of WCE was resolved on 4-12% NOVEX gels using MOPS buffer (Invitrogen). Protein was transferred to PVDF membrane (Invitrogen) and blotted for BRCA1 (D9, Santa-

Cruz); BCLAF1 (BTF 608A, Bethyl Labs); U2AF65 (MC3 or H300, Santa-Cruz); Prp8 (E5, Santa-Cruz); YB1 (59-Q, Santa-Cruz); BACH1 (4578 Cell Signalling); ATRIP (H300 Santa-Cruz); Exo1 (N18 Santa-Cruz), γ-Tubulin (GTU-88 Sigma).

Quantification of Protein Turnover

Western blots were carried out as indicated above form cells treated with cyclohexamide for increasing time-points in the absence or presence of DNA damage. Image densitometry was carried out using image-J and quantified protein levels were normalised to those quantified in cells harvested immediately after cyclohexamide treatment (0hrs). Normalised protein levels were then plotted and one-phase exponential decay curves fitted using Graphpad Prism. These curves were then used to calculate protein half-lives (t1/2).

Chromatin Immunoprecipitations (ChIP)

Chromatin was cross- linked using 1.5% formaldehyde for 15 minutes at room temperature. Cells were then washed twice with PBS and collected in 1 mL collection buffer [100mM Tris-HCL (pH 9.4) and 100mM DTT]. The cell suspension was then incubated on ice for 15 minutes. Cells were then lysed sequentially by resuspension and 5-minute centrifugation at 3,000g at 4^{o}C with 1 mL buffer A (10mM EDTA, 0.5mM EGTA, 10mM HEPES, and 0.25% Triton X-100) and 1 mL buffer B (1mM EDTA, 0.5mM EGTA, 10mM HEPES, and 200mM NaCl), and sonicated three times for 10 seconds at maximum settings in 250 mL lysis buffer (10mM EDTA, 50mM Tris-HCl, 1% SDS, and 0.5% Empigen BB). After 15-minute centrifugation, 10 ML of the supernatant was taken as input and the remainder was diluted 5-fold in immunoprecipitation buffer (2mM EDTA, 100mM NaCl, 20mM Tris-HCl, and 0.5% Triton X-100). This was then subjected to immunoprecipitation overnight with specific antibodies after preclearing with pre-immune IgG, 2mg salmon sperm DNA, and 60mL protein A/G Sepharose bead slurry. Precipitate complexes were serially washed with 300 mL washing buffer I (2mM EDTA, 20mM Tris-HCl, 1% SDS, 01% Triton X-100, and 150mM NaCl), washing buffer II (2mM EDTA, 20mM Tris-HCl, 1% SDS, 01% Triton X-100, and 250mM NaCl), washing buffer III (1mM EDTA, 10mM Tris-HCl, 1% NP40, 1% deoxycholate, and 0.25M LiCl) then twice with 1 mM EDTA and 10mM

Tris-HCl. Complexes were removed from the beads through subsequent 15-minute incubations, vortexing, and 5-minute centrifugations with 50 ML of 1% SDS, 0.1 mol/L NaHCO3. Cross-linking was reversed overnight at 65°C and the DNA was purified with QIAquick columns (Qiagen). Antibodies used for ChIP were BRCA1 (Ab-1; Calbiochem), HA (sc-805, Santa Cruz), and BCLAF1 (BTF 608A Bethyl Labs), and anti-rabbit/mouse IgG (DAKO). qPCR was performed on ChIP derived DNA using the following primers:

Fold enrichment was calculated by first normalising to input qPCR and then normalising to the same normalised value calculated for the same ChIP using primers specific to a control region ~2kp upstream of the S100A7 TSS. (Primers:

RNA-Immunoprecipitations (RIP)

Cells were fixed with 1% PFA/PBS to crosslink protein bound DNA/RNA complexes. Cells were then washed, lysed and Nuclei and chromatin extracts were prepared as described above (ChIP assay) with all buffers containing RNaseOUT (Invitrogen). Samples were then sonicated to produce DNA/RNA fragments of approx 500 bp (as analysed by electrophoresis). Antibodies used for immunoprecipitation were BRCA1 (Ab-1;Calbiochem), BCLAF1 (BTF 608A, Bethyl Labs); U2AF65 (H300, Santa-Cruz); rabbit IgG and IgG1 (DAKO), HA (Y11 Santa-Cruz). The sonicated extract was split into equal aliquots, made up to a total of 1.3 ml with IP buffer (1%Triton X100, 0.1% DOC, 1X TE, RNaseOUT) and 50 ul of the Dynabead/antibody complex added per IP, and allowed to incubate overnight at 4°C. The RIPs were washed x6 using the magnetic particle concentrator (MPC) with RIPA buffer (50 mM Hepes pH 8, 1mM EDTA, 1% NP40, 0.7% DOC, 0.5M LiCl and protease inhibitor mix, RNaseOUT), and once with 1X TE buffer. The DNA/RNA was extracted from the beads twice, by addition of 50 ul of elution buffer (10mM Tris pH 8, 1mM EDTA, 1%SDS, RNaseOUT), and incubation at 65°C, with vortexing every 2 min. To reverse the crosslinking, samples were made up to a total volume of 170 ul and incubated for 5hrs at 70°C, in a tube with a hole in the lid to allow evaporation. After reverse crosslinking, 500 ul of STAT60 (AMSBIO) was added per sample and RNA extracted as per manufacturers instructions. DNAse I treatment (roche) was

performed as per manusfacturer protocol, and cDNA was synthesised using the Transcriptor High Fidelity cDNA Synthesis Kit (Roche Applied Science). 3 ul of cDNA was then used per qPCR (Roche Lightcycler 480) using primers indicated above.

ChIP-chip and analysis

Three independent BCLAF1 ChIPs were performed from 293T cells transfected with siCtrl or siBRCA1 siRNAs and either mock treated or treated with 1μM Etoposide for 16hrs. Purified BCLAF1-ChIP derived and total input DNA for each sample was amplified using the whole genome amplification kit (sigma Aldrich) as directed by NimbleGen protocols (see http://NimbleGen.com for details). 4 mg of immunoprecipiated and total DNA was shipped to NimbleGen Systems for labelling and array hybridisation on NimbleGen Human ChIP-chip 3x 720K Human RefSeq Promoter array. This array covers 30,893 transcripts (3200 bp upstream tiling, 800 bp downstream tiling, probes are spaced approximately 100bp apart). The two colour array data from input Vs BCLAF1-ChIP was normalised using MA2C hosted on Cistrome (Liu et al., 2011; Song et al., 2007). The NimbleGen 3x 720K Human RefSeq Promoter array design (*.ndf) and position (*.pos) files were uploaded to Cistrome along with the raw probe signal files and MA2C used to normalise raw probes signals and call binding peaks. Peak calling and normalisation was carried out using the following MA2C settings: Bandwidth = 500, Max Gap = 250, Minimum probes = 4 , Threshold method = Pvalue with p-value of 0.005, Normalization method = robust with c value = 2. Lists of BCLAF1 binding peaks were generated by overlapping binding regions from replicate ChIPs and identifying regions bound in at least 2 of 3 replicate experiments. Genes only bound by BCLAF1 in etoposide treated cells were then identified for siCtrl and siBRCA1 transfected cells. Genes only bound by BCLAF1 in the presence of BRCA1 were then identified by overlapping the etoposide treated siCtrl, BCLAF1 bound gene list with the etoposide treated siBRCA1, BCLAF1 bound genelist **(Figure S3a)**.

DNA Repair Assays

Cells were transfected with siRNAs and incubated for 24hrs. Cells were then plated onto coverslips and incubated for a further 24-48hrs (depending on the post-treatment time point required) before treatment with 2Gy IR using an X-RAD 225 X-ray generator (Precision X-ray Inc. Branford, CT, USA) at a dose rate of 0.591 $Gy.min^{-1}$. Cells were fixed at 0 and 24hrs post IR in 4% paraformaldehyde/PBS and then permeabilised in 0.2% Triton X-100/PBS followed by blocking in 3% BSA/PBS. Cells were then stained with anti-γ-H2AX primary antibody (Millipore 05–636) and anti-mouse AlexaFluor 486 (Invitrogen) secondary antibody. Cells were also counterstained with DAPI to identify cellular nuclei. Cells containing more than 5 γ-H2AX foci were scored and representative images acquired using a Nikon Eclipse Ti-S fluorescence microscope, with 60x objective.

Immunofluorescence microscopy

Cells were grown on cover slips and treated as indicated. Following indicated time points cells fixed in 4% paraformaldehyde/PBS and then permeabilised in 0.2% Triton X-100/PBS followed by blocking in 3% BSA/PBS. Cells were then stained with primary antibodies; anti BCLAF1 (Bethyl Labs A300-608A (1:2000)), U2AF65 (Santa-Cruz MC3 (1:500)) or γ-H2AX (Millipore 05–636 (1:10, 000)). Cells were then stained with AlexaFluor-486 or 568 (Invitrogen) and counterstained with DAPI to identify cellular nuclei. Cells were imaged on a Nikon Eclipse Ti-S fluorescence microscope, with 60x objective.

Immunofluorescence microscopy with pre-extraction of non-chromatin proteins for visualisation of chromatin bound pS1423-BRCA1.

Cells were transfected with control and BRCA1 siRNAs using Lipofectamine RNAiMAX as per manufacturers instructions and plated on coverslips. 72 hours following transfection cells were treated with 2Gy IR. One hour following IR cells were treated with extraction buffer (20 mM Hepes, 20 mM NaCl, 5 mM MgCl2, 1 mM ATP, 0.5% IGEPAL (same chemically as obsolete Nonidet P-40), pH 7.5), supplemented with complete mini protease inhibitor (Roche) and PhoStop phosphatase inhibitor (Roche) as per manufacturers instructions)), on ice for 20 min after which cells were fixed with 4% paraformaldehyde in PBS. Cells were

then blocked with 3% BSA/PBS and stained with γ-H2AX (Millipore 05–636 (1:10, 000)) and pS1423-BRCA1 (Bethyl Laboratories (A300-008A) 1:500)) antibodies.. Cells were then stained with AlexaFluor-486 or 568 (Invitrogen) and counterstained with DAPI to identify cellular nuclei. Coverslips were mounted with ProLong Gold mounting agent (LifeTechnologies) and imaged using a Leica SP5 confocoal microscope.

Laser microirradiation

Cells grown on glass-bottom dishes (Willco Wells) in phenol red-free complete medium (Invitrogen) were presensitized with 10 μM bromodeoxyuridine (BrdU) for 24 hr. Laser microirradiation was performed by a FluoView 1000 confocal inverted microscope (Olympus) equipped with a 37°C heating stage (Ibidi) and a 405 nm laser diode (6 mW) focused through a 60× UPlanSApo/1.35 oil objective to yield a spot size of 0.5–1 μm. The time of cell exposure to the laser beam was approximately 250 ms (fast scanning mode). The laser settings (0.40 mW output, 50 frames) were chosen to generate a detectable damage response restricted to the laser path in a presensitization-dependent manner without noticeable cytotoxicity. Cells were fixed and analyzed by immunofluorescence 20 min after microirradiation unless indicated otherwise.

Metaphase Spreads and Chromosomal Aberration Analysis

Cells were transfected with siRNAs (siCtrl, siBRCA1 and siBCLAF1) and incubated for 48hrs. Cells were then mock irradiated or irradiated with 2Gy IR using an X-RAD 225 X-ray generator (Precision X-ray Inc. Branford, CT, USA) at a dose rate of 0.591 $Gy.min^{-1}$. Twenty hours after irradiation cells were treated with Colcemid (0.4μg/mL 293Ts and 0.2μg/mL MCF7s) for a further 4hrs after which cells were trypisinized and spun down. Metaphases were collected by resuspending pellet with hypotonic 75 mM KCl for 20 min at 37 °C, followed by fixation for 20 min at 4 °C in freshly prepared Carnoy solution (3 : 1 v/v methanol/acetic acid). After two more washes in Carnoy solution, cells were dropped onto pre-warmed wet slides and air-dried at room temperature and aged at room temperature for 7 days. Aged slides were hybridised with whole-chromosome fluorescence-labelled DNA probes (XCP, Whole-Chromosome

Probe, MetaSystems) directed to chromosomes 1 (fluorochrome FITC) and chromosome 2 (fluorochrome Texas Red) as per manufacturer's instructions. DNA denaturation (72 °C for 3 min) and hybridisation (37 °C for 8 hr) were performed using the HYBrite chamber system (Vysis). All chromosomes were counterstained with DAPI (Sigma). Coded slides were viewed with an epi-fluorescence microscope (Axioplan2 imaging MOT, Carl Zeiss) connected to an automated system (Metafer 4 software, MetaSystems) for slide scanning and three-colour image acquisition. Chromasome aberrations were analysed on stored images. All slides were scored blind by the same scorer. All types of aberrations were scored separately and categorised in simple exchanges (i. e. translocations and dicentrics), either visibly structurally complete or incomplete, acentric excess fragments and complex exchanges. No centromere probe was used but centromeres were clearly distinguishable as bright bands under DAPI illumination.

ATM and ATR inhibition

Cells were pre-treated with 10μM each of ATM inhibitor (KU55933, tocris bioscience) and ATR inhibitor (ATRi a kind gift from Dr. Oscar Fernandez Capetillo, Spanish National Cancer Research Centre, Madrid, Spain).

Analysis of publically available BRCA1 ChIP-Seq data

BRCA1 chip-seq .wig files were downloaded from GEO accession No. GSE40591. Peaks were called using the general peak caller version 1.0.0 implemented in the Cistrome Galaxy instance (Liu et al., 2011). The resulting bed and .wig files were analysed utilising the Cis-Regulatory Element Analysis System (CEAS) (Shin et al., 2009), which tests for statistical enrichment of peaks relative to a range of genomic features and also plots the average genome wide ChIP-seq profiles with respect to a range of these features. The integrative Genomics Viewer (IGV) genome browser was used to visualize binding across the ATRIP, BACH1 and EXO1 genes (Thorvaldsdottir et al., 2013).

References

Liu, T., Ortiz, J.A., Taing, L., Meyer, C.A., Lee, B., Zhang, Y., Shin, H., Wong, S.S., Ma, J., Lei, Y.*, et al.* (2011). Cistrome: an integrative platform for transcriptional regulation studies. Genome Biol *12*, R83.

Shin, H., Liu, T., Manrai, A.K., and Liu, X.S. (2009). CEAS: cis-regulatory element annotation system. Bioinformatics *25*, 2605-2606.

Song, J.S., Johnson, W.E., Zhu, X., Zhang, X., Li, W., Manrai, A.K., Liu, J.S., Chen, R., and Liu, X.S. (2007). Model-based analysis of two-color arrays (MA2C). Genome Biol *8*, R178.

Stucki, M., Clapperton, J.A., Mohammad, D., Yaffe, M.B., Smerdon, S.J., and Jackson, S.P. (2005). MDC1 directly binds phosphorylated histone H2AX to regulate cellular responses to DNA double-strand breaks. Cell *123*, 1213-1226.

Thorvaldsdottir, H., Robinson, J.T., and Mesirov, J.P. (2013). Integrative Genomics Viewer (IGV): high-performance genomics data visualization and exploration. Brief Bioinform *14*, 178-192.